Yukon

YGS Open File 2023-3

Analysis of geoscience data for geothermal exploration along the Teslin fault near Teslin, Yukon

J.B. Witter

Yukon

YGS Open File 2023-3

Analysis of geoscience data for geothermal exploration along the Teslin fault near Teslin, Yukon

J.B. Witter
Innovate Geothermal Ltd.

innovate Geothermal

Published under the authority of the Department of Energy, Mines and Resources, Government of Yukon https://yukon.ca/en/department-energy-mines-resources.

Whitehorse, Yukon, 2023.

Publié avec l'autorisation du Ministères de l'Énergie, des Mines et des Ressources du gouvernement du Yukon, https://yukon.ca/en/department-energy-mines-resources.

Whitehorse (Yukon) en 2023.

This, and other Yukon Geological Survey publications, may be obtained from:
Yukon Geological Survey
102-300 Main Street
Box 2703 (K-102)
Whitehorse, Yukon, Canada Y1A 2C6
email geology@gov.yk.ca

Visit the Yukon Geological Survey website at https://yukon.ca/en/science-and-natural-resources/geology.

In referring to this publication, please use the following citation:

Witter, J.B, 2023. Analysis of geoscience data for geothermal exploration along the Teslin fault near Teslin, Yukon. Yukon Geological Survey, Open File 2023-3, 48 p. plus digital appendices.

Front cover: Looking south at Teslin Lake and the Village of Teslin from communication tower north of Fox Creek. Dawson Peaks in the background, across the lake. Photo credit: Rosie Cobbett, YGS.

Table of Contents

Abstract

In collaboration with the Yukon Geological Survey, Teslin Tlingit Council, and other project partners, Innovate Geothermal Ltd. performed an analysis of geoscience data in south-central Yukon as part of an effort to better understand the potential for geothermal energy resources that, if present, could be utilized to help reduce fossil fuel use in Yukon communities. The study area for this project is located near the Village of Teslin and straddles the Teslin fault zone. The main aim of this project is to analyze and interpret a variety of pre-existing and newly acquired geologic and geophysical data sets to evaluate whether geothermal reservoirs may be present within the study area. A secondary aim is to propose favourable drilling locations, if warranted, for exploratory wells to collect information on subsurface temperature and permeability. The geoscience work accomplished here includes both 2D map interpretation as well as construction of a 3D geologic model that was guided by geophysical inversion modelling of gravity and magnetic survey data. In the Teslin study area, the distribution of temperature in the subsurface remains a significant unknown; however, limited evidence suggests subsurface temperatures are modestly above average. Specifically, regional-scale, Curie point depth estimates suggest the geothermal gradient in the area is ~45 °C/km. Drilling is required to measure actual subsurface temperature gradients in the vicinity of Teslin. Furthermore, subsurface permeability does appear possible in the study area. Analysis of the geoscience data shows evidence for a complex structural environment that appears favourable for subsurface fracture permeability in the Teslin fault zone area. In addition, geologic mapping and geophysical modelling suggests that large portions of the Teslin study area are underlain by quartzite and volcanic bedrock. Both rock types have a favourable potential for maintaining open fractures. Many unknowns regarding the temperature and permeability of the subsurface still exist in the Teslin study area. The location of a 500 m deep scientific research well is proposed to help answer many of the remaining questions.

Introduction

Teslin is a small community in south-central Yukon which obtains energy from a 25 kV electric transmission line connected to Whitehorse, a 1.5 MW diesel generating station, a 1 MW biomass (wood chip) district heating system, as well as the burning of fossil fuels or wood to heat individual buildings (Government of Yukon, 2018). Replacing the fossil fuel power generation with clean, renewable power would significantly reduce greenhouse gas emissions from Teslin and free the community from the uncertainty associated with the cost of diesel. Energy derived from subterranean geothermal reservoirs in the Teslin area could be beneficial in two different ways: 1) warm water from lower temperature (< 100 °C) geothermal reservoirs could be tapped to directly heat buildings, thereby reducing the amount of fossil fuel and biomass needed for space heating; and 2) hot water from higher temperature (> 100 °C) geothermal reservoirs could be utilized to generate electricity to directly replace fossil fuel power generation.

Existing geoscience data (although limited) suggests that there are above average subsurface temperatures in the Teslin region. However, for a natural subsurface geothermal reservoir to be tapped, there also needs to be permeability (*e.g.*, fractures) in the subsurface that allow the geothermal fluids to flow through the rock into the wellbore of a geothermal production well. One possible location of fractured rock and permeability is the Teslin fault, a major crustal structure with multiple strands that runs northwest-southeast near the Village of Teslin (Fig. 1). Unfortunately, our geologic understanding of the Teslin fault is incomplete, due to a lack of detailed geoscience

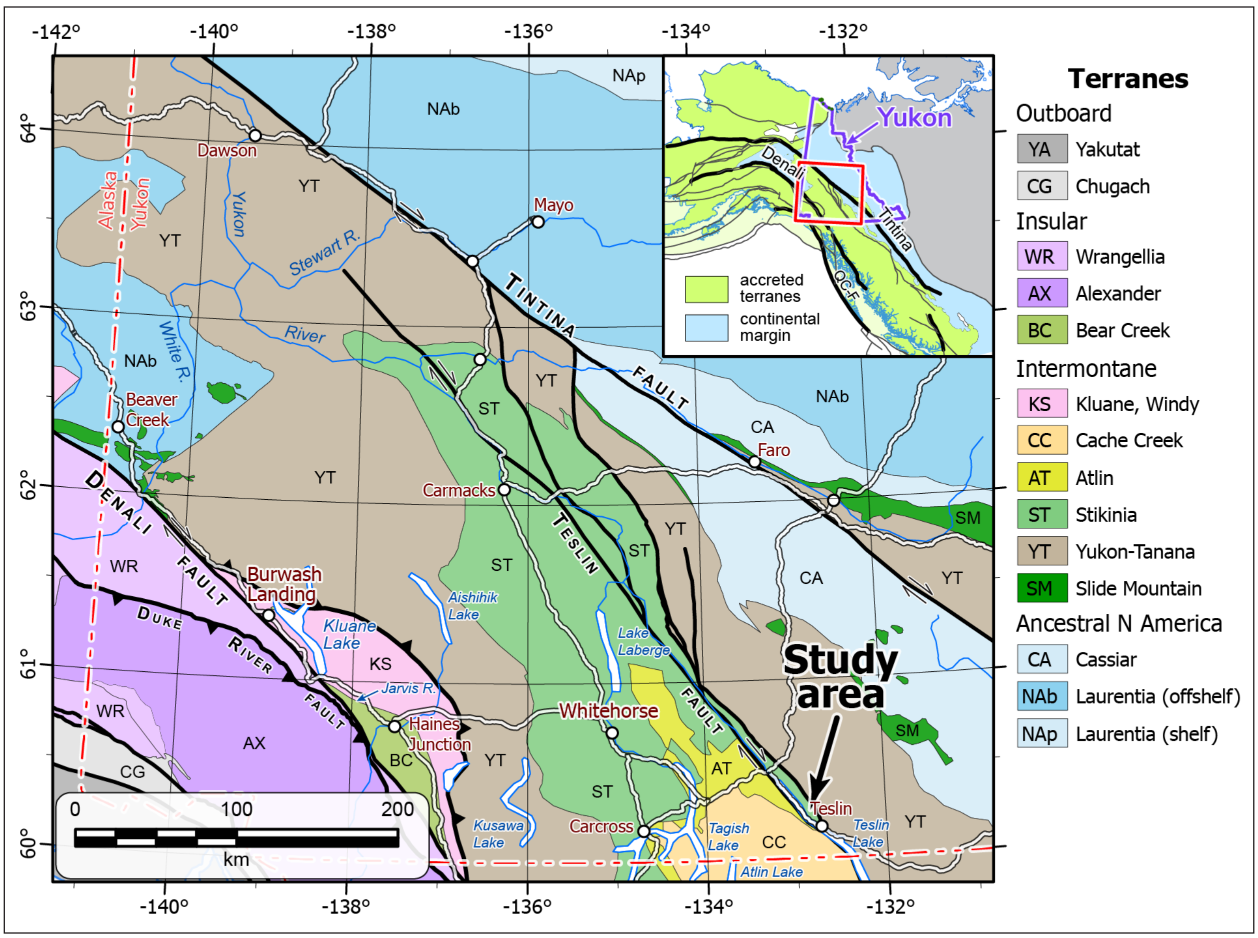

Figure 1. *Map of Yukon illustrating the location of the study area described in this report. Geologic terrane basemap from Yukon Geological Survey (2023a). Black lines depict major faults. Red dashed lines show provincial/territorial borders.*

investigations in the Teslin area coupled with an absence of deep drilling near the Teslin fault.

Therefore, the purpose of this study is to obtain and interpret baseline geoscience data in the Teslin area to:

1. Better constrain the location, strike and dip of the Teslin fault and associated fault structures;
2. develop a 3D geologic framework for the Teslin subsurface to infer the locations of potentially permeable fault structures; and
3. better understand the geometry and composition of major rock units that may or may not host geothermal reservoirs.

The specific study area for this project is ~10 km wide and ~10 km long, straddles the Alaska Highway, and is approximately centered on the Village of Teslin (Fig. 2). Three-dimensional geoscience modelling was performed to try to extend our understanding of the study area to a depth of ~4.5 km below the ground surface. Such an exercise can be useful because the presence or absence of geothermal fluid reservoirs can be dependent on both rock type and geologic structures. Thus, having some idea of the location of specific rock types, as well as the location of faults in the subsurface, is valuable in the search for geothermal resources. To achieve these goals, existing geoscience data from the study area were compiled and interpreted alongside new geoscience data which were acquired as part of this project. These data are described in this report.

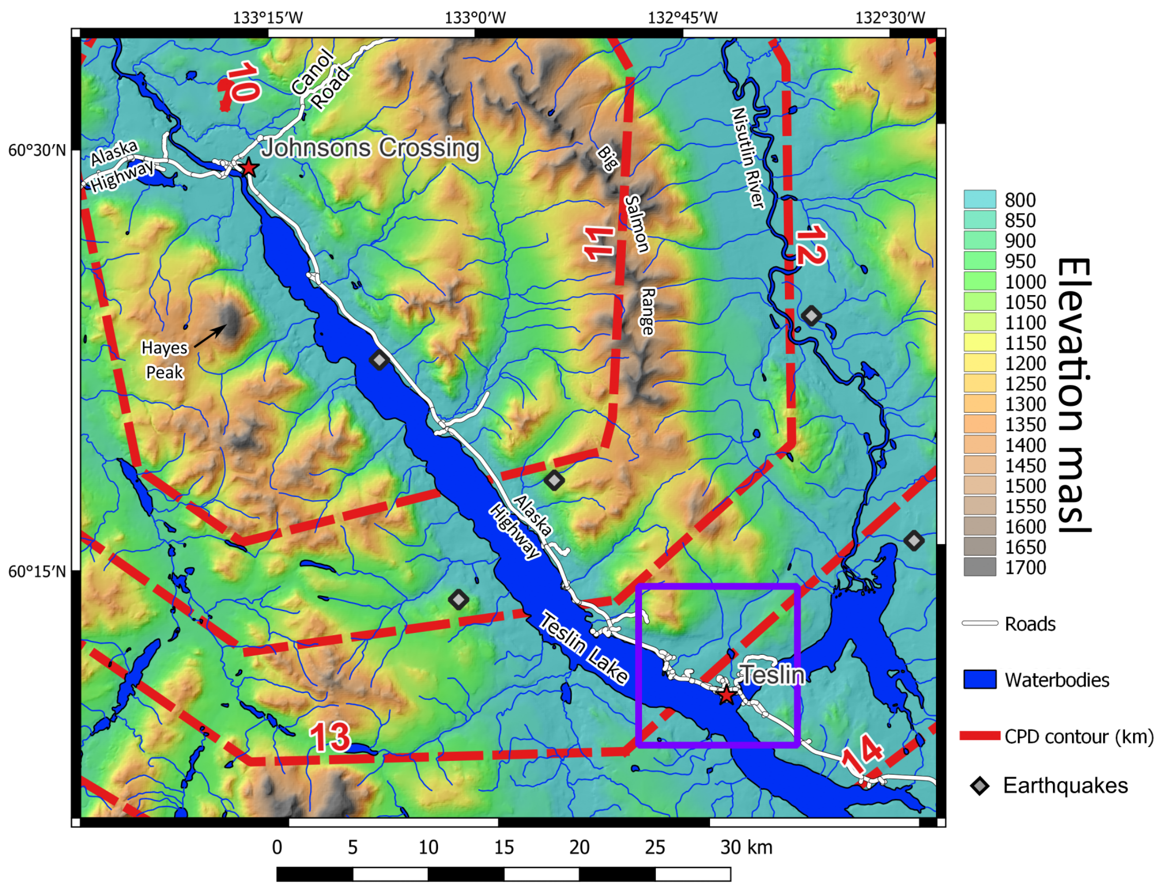

***Figure 2.** Topography in the Teslin area from CDED data with the ~10 km x ~10 km study area outlined in purple. Curie point depth contours (red dashed lines) are labelled in kilometres. Historic earthquake epicentres are also shown (grey diamonds).*

Background

Typical indicators of geothermal resources (*e.g.*, hot springs and active volcanism) are absent in the Teslin study area. However, there is evidence for above average subsurface temperatures at a regional scale. Furthermore, a major fault zone cuts through the study area suggesting the possible presence of fractured, permeable rock in the subsurface. Background information on these topics is summarized here.

Curie point depth estimate

Curie point depth (CPD) mapping has been used as an initial exploration tool in Yukon to help identify warm vs. cool crustal temperatures in the territory (Witter *et al.*, 2018). Curie point depth mapping is a method, originally developed in the 1970s, which uses regional-scale magnetic survey data to map the depth to the Curie point temperature (~580 °C) where magnetization in rocks disappears. Regions found to have shallow CPD values are expected to have higher heat flow, higher average thermal gradient, and therefore, a higher likelihood of geothermal energy resources that are accessible via drilling. Curie point depth values calculated for the Teslin study area are estimated to be ~13 km (Li *et al.*, 2017; Witter *et al.*, 2018; see Fig. 2) which translates into an average, crustal-scale temperature gradient of ~45 °C/km. Such a thermal gradient is modestly higher than the average thermal gradient of the Earth's crust (~25-30 °C/km). If these estimates are accurate, a 2 km borehole in the Teslin area could be expected to reach ~90 °C.

Bedrock and surficial geology

Regional scale bedrock geology of the Teslin area (Fig. 3) can be summarized as follows (from Colpron, 2022; Gordey and Stevens, 1994):

- Neoproterozoic to Paleozoic metamorphic rocks of the Yukon-Tanana terrane lie to the northeast of the Teslin fault zone;
- Mesozoic mafic volcanic rocks as well as clastic sedimentary and carbonate rocks of the Cache Creek terrane lie to the southwest of the Teslin fault zone;
- a several kilometre-wide sliver of Mesozoic sedimentary and volcanic rocks of the Quesnellia terrane is sandwiched between two northwest-trending, sub-parallel strands of the Teslin fault;
- a narrow sliver of Mesozoic volcanic rocks of the Atlin terrane lies between the Quesnellia and Cache Creek terranes; and
- the elongate, Early Cretaceous, Deadman Creek pluton (granite/granodiorite) parallels the Teslin fault zone and flanks its northeast side.

Within the Teslin study area, the bedrock units present include (Fig. 3):

- Neoproterozoic-Paleozoic metamorphic rocks (mostly quartzite) of the Snowcap assemblage and Paleozoic metavolcanic rocks of the Finlayson assemblage which lie east of the Teslin fault in the study area (Yukon-Tanana terrane);
- Triassic-Jurassic volcanic rocks of the Shonektaw Formation (Quesnellia terrane) that occur east of Teslin Lake between the two strands of the Teslin fault;
- Triassic basalt of the Nakina Formation (Atlin terrane; Zagorevski *et al.*, 2021) exposed along the southern shore of Teslin Lake;
- Triassic-Lower Jurassic sedimentary rocks of the Cache Creek terrane (mostly chert and shale) in the southwest corner of the study area; and
- granitic rocks of the Deadman Creek pluton lie in the northeast corner of the study area.

Surficial geologic mapping (Yukon Geological Survey, 2020; Morison and Klassen, 1997) shows that the Teslin study area is largely covered by a blanket of glacial deposits. Bedrock is exposed mostly in restricted localities, such as on high ridges that have been scoured by glaciers. Surficial geologic data is helpful for identifying portions of the study area most likely to host thicker sections of recent, low-density sediments, such as the Fox Creek valley.

Teslin fault and other geologic structures

Faults within the Teslin study area include: 1) the northwest-trending, strike-slip, right-lateral Teslin fault zone; and 2) a thrust fault which forms the boundary between the Atlin and Cache Creek terranes along the southern shore of Teslin Lake (Fig. 3). The most important of these is the Teslin fault zone, a major structure that marks the boundaries between different terranes. The southern strand of the Teslin fault is obscured by Teslin Lake, but it is demarcated based upon different rock types on either side of the lake. Other portions of the Teslin fault are not exposed but the fault location is well-constrained by contrasting rock types (Gordey, 1991). The Teslin fault zone is the northern extension of the Thibert-Kutcho fault zone in northern British Columbia where an estimated ~130 km of dextral strike-slip movement occurred (Gabrielse *et al.*, 2006; Mihalynuk *et al.*, 2006).

In addition to the significant amount of displacement, the Teslin fault zone is of interest because it bifurcates into two northwest-trending fault strands at a point several kilometres southeast of the Village of Teslin. Fault bifurcation has been recognized at other dextral fault zones (e.g., the Sumatran fault; Sieh and Natawidjaja, 2000) and is often associated with structurally complex strike-slip duplexes (Woodcock and Fischer, 1986). These observations about the Teslin

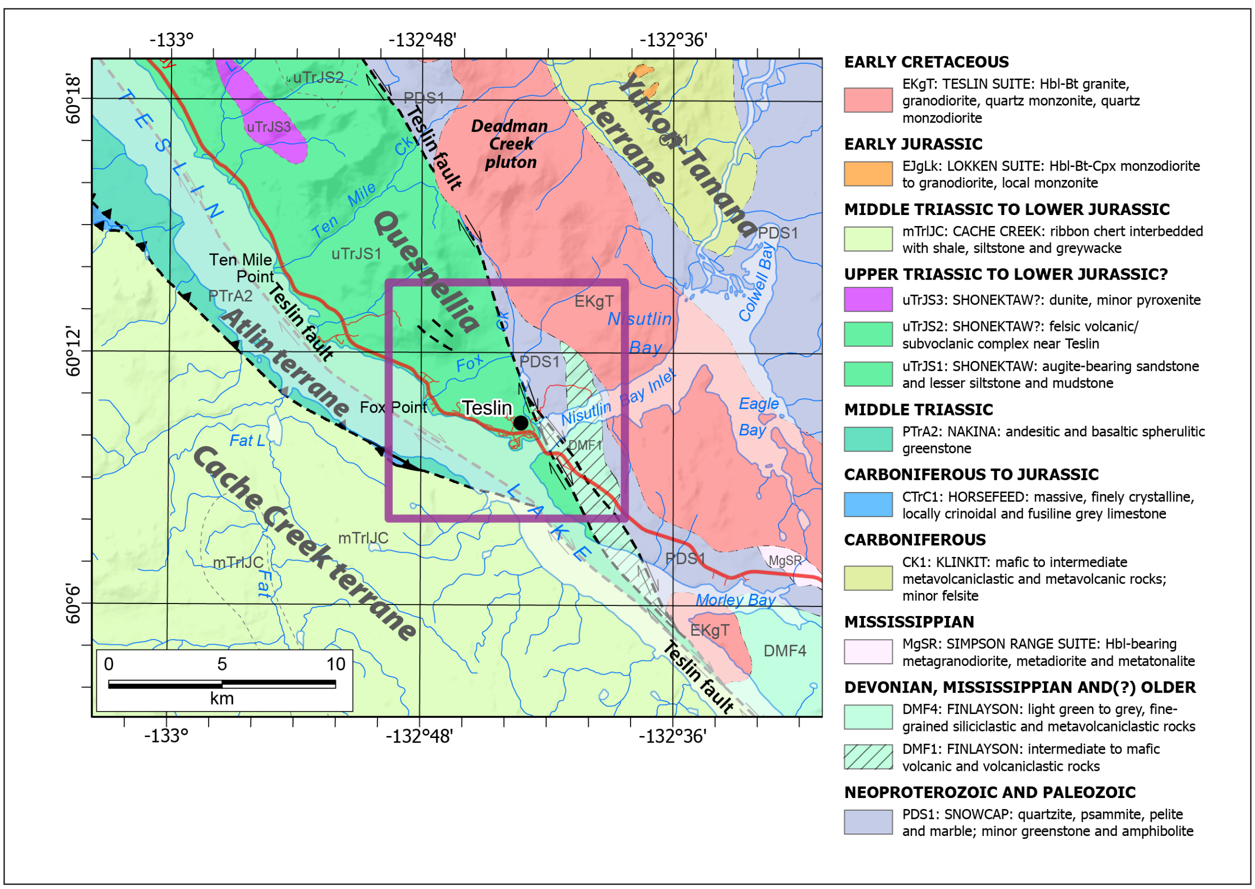

Figure 3. *Bedrock geology in the Teslin area, Yukon (adapted from Colpron, 2022 and Yukon Geological Survey, 2023b). The study area is shown by the purple square.*

fault zone suggest that the subsurface in the vicinity of the Village of Teslin is also a structurally complex region that could potentially host faulted and fractured, permeable rock.

The Teslin fault zone appears to be currently inactive. It is not mentioned by Leonard *et al.* (2008) who presented a summary of fault deformation rates in the northern Canadian Cordillera. Some researchers suggest that significant deformation along the Teslin fault had ended by the Late Cretaceous or early Tertiary (Larson, 2002; Mihalynuk *et al.*, 2006; White *et al.*, 2012).

Heat flow data

Only one heat flow datapoint obtained from mineral exploration boreholes (Lewis *et al.*, 2003) is available within ~100 km of the Village of Teslin. The Ruby Creek mine, located ~60 km southwest of Teslin in British Columbia, has a reported heat flow of 98 mW/m^2. Globally, the mean heat flow over continental crust is only 65 mW/m^2. Thus, regional heat flow for the Teslin region is elevated.

Deep well data

According to public records, no deep wells (*i.e.*, > 200 m) have been drilled in this part of Yukon.

Radiogenic heat production data

There are many direct estimates of radiogenic heat production from plutons located in the region around Teslin (Colpron, 2019; Colpron *et al.*, 2021). Most of these estimates, however, are similar to or less than the global average value for heat production in granites (2.5 – 2.8 $\mu W/m^3$; Hasterok and Webb, 2017).

For example, the Early Cretaceous Deadman Creek pluton (Fig. 3), that lies ~10 km northeast of Teslin Lake, yields five rather modest heat production values in the range of 0.9–2.9 $\mu W/m^3$. Only two samples from the far northern end of the Deadman Creek pluton (~40 km from the Teslin study area) returned elevated values (4.5–5.0 $\mu W/m^3$). The Early Cretaceous Strawberry Creek pluton (which lies ~20 km east of the Teslin study area) also exhibit modest heat production values of 2.3–3.1 $\mu W/m^3$. One exception to this trend is the Early Cretaceous Wolf pluton, located ~20 km northeast of the Teslin study area, for which one sample has a very high heat production value of 11.4 $\mu W/m^3$ (Colpron *et al.*, 2021). On the west side of Teslin Lake, the Early Cretaceous Hayes Peak pluton (Fig. 2) has two heat production values in the range 0.1–3.4 $\mu W/m^{3.}$ In addition, the Jurassic age Mt. Bryde pluton, located ~20 km west of the Teslin study area has rather low heat production values in the range of 0.9–1.6 $\mu W/m^3$. Based upon these data, radiogenic heat production is not expected to be a significant heat source for geothermal reservoirs in the Teslin area.

Earthquake data

Data on earthquake epicenters for the Teslin area were obtained from the NRCAN (https://earthquakescanada.nrcan.gc.ca/). Five historic earthquakes are reported within a 50 km x 50 km area around Teslin (Fig. 2). These quakes occurred between 1997 and 2013 with magnitudes ranging from 1.5 to 2.4 and depths between 1 and 95 km. Only three of the reported earthquake epicenters lie within 5 km of the Teslin fault zone; none of them lie within the Teslin study area. The small number and magnitude of historic earthquakes in the Teslin region is consistent with geologic observations which suggest a lack of recent fault movement in the area.

Favourable structural environments

For geothermal fluids to flow in the subsurface, faults and fractures need to be abundant and permeable. Studies from southern Yukon show that the tectonic regime in the area is under compression in a direction oriented approximately northeast-southwest (Hyndman *et al.*, 2005). Compressional conditions in the crust tend to close fractures and inhibit subsurface fluid flow.

However, the observed bifurcation in the Teslin fault zone may have generated an abundance of complex fault structures, in the form of a strike-slip duplex (Fig. 4), that create a significant volume of permeable and fractured rock that could host warm geothermal fluids. Similarly, extensional pull-apart basins associated with strike-slip duplex structures could play a key role in creating subsurface permeability like what has been observed along the Sumatra fault in Indonesia (Sutrisno *et al.*, 2019).

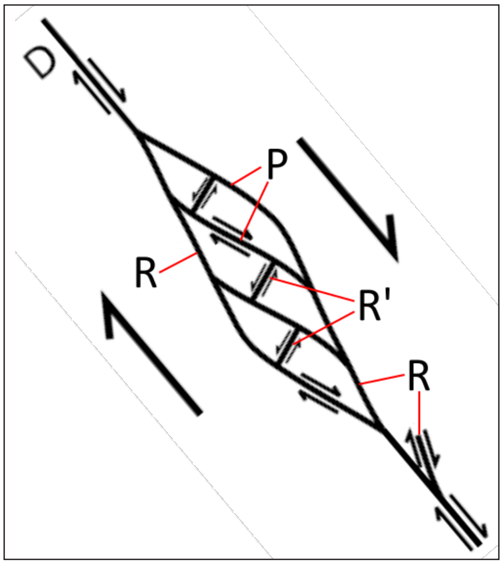

Figure 4. *An example of a strike-slip duplex geometry that could form within a bifurcating strike-slip fault zone (adapted from Weller et al., 2012). The labels P and D represent a shear that forms at high displacement; R and R' are conjugate Riedel shears with a different orientation that form at low displacement (Woodcock and Fischer, 1986). The R' Riedel shears can accommodate sinistral movement (as shown here) as well as extensional motion to form small pull-apart basins. This schematic diagram represents structures that may exist in association with the Teslin fault zone. For example, similar to the diagram above, the Teslin fault zone is bifurcated, has a northwest strike, and dextral motion.*

Geothermal exploration summary and strategy

What do we know?

Existing geoscientific information in the project area, outlined in the previous section, suggests the following:

- an above average crustal thermal gradient of ~45 °C/km may be present in the Teslin study area, based upon Curie point depth mapping;
- a single datapoint suggests that regional heat flow is high in the Teslin area, on the order of ~100 mW/m^2;
- the tectonic regime along the Teslin fault is a transpressive environment which exhibits right-lateral strike-slip fault motion;
- the Teslin fault is likely inactive at the present time;
- earthquake activity is very low along the Teslin fault and, thus, may contribute little to present-day creation of open fractures (*i.e.*, permeability) in the subsurface in the study area;
- the Teslin fault zone bifurcates into two strands that may form a complexly fractured and potentially permeable subsurface environment near the Village of Teslin; and
- one specific structural environment that could be favourable for geothermal fluid upwelling (if present) along the Teslin fault zone is a strike-slip duplex with extensional pull-apart basins; such a structural environment is key to the existence of geothermal systems along a similar fault zone in Sumatra (Sutrisno *et al.*, 2019).

What do we want to know?

In any geothermal exploration program, the two key requirements for a viable geothermal resource are elevated temperature and adequate rock permeability. Subsurface temperatures in the uppermost few kilometres of the Earth's crust can only be known accurately via downhole measurements in wells. At this time, the absence of deep wells near the study area limits understanding of subsurface temperatures to estimates inferred from the Curie point depth map (Fig. 2). We can, however, attempt to identify where fractured and permeable rocks may be present in the subsurface by using geologic and geophysical data. By doing so, we can infer where geothermal fluid upwelling might be possible. In the Teslin area, permeability could be associated with crustal scale fractures along faults that would promote deep (*i.e.*, several kilometres) meteoric water circulation and allow heat from depth to rise to the surface. For this study, there are important questions to address:

1. Is there a complex network of faults associated with the fault bifurcation in the Teslin fault zone? If so, where are they and what is their orientation?
2. Is there specific evidence for a strike-slip duplex associated with the Teslin fault zone within the project area? If so, where?
3. Where in the subsurface are the rock types that are more prone to sustain open fractures, and what is their spatial distribution?

In order to begin to address these questions, a more thorough understanding of the 3D geologic and structural framework of the subsurface is required. Thus, a significant amount of the effort in this study is aimed at building a 3D geoscience model of the lithology and faults within the project area. The overall goal is that the 3D geoscience model, generated for this project, can serve as a guide for selecting drilling targets that would give direct characterization of the bedrock and measurements of subsurface temperature and permeability. The next sections describe the data and methods used in our attempt to create a 3D geoscience model that is consistent with all the various geoscience datasets available.

Data used in this project

Existing geoscience data

Topographic data

Topographic data compiled in the Teslin region include: CDED data (16 m resolution), Arctic DEM data (as good as 2 m resolution), and LiDAR data (~1 m resolution; made available by the Yukon Geological Survey). Unfortunately, Arctic DEM data contain kilometre sized holes in it near the Village of Teslin and the LiDAR data covers only ~60% of the Teslin study area. To create the best possible topographic dataset for the study area, the LiDAR data was given priority and then supplemented by Arctic DEM and CDED data, as needed, to fill in gaps to create a new DEM. This topographic stitchwork was performed by Aurora Geosciences as part of their gravity survey effort (Appendix 3). Elevation in the Teslin study area ranges from ~700 m above sea level (masl) at Teslin Lake to ~1400 masl in the hills of the Big Salmon Range at the northwest corner of the study area (Fig. 5).

Water well data

A substantial amount of subsurface information from water wells is available for the Teslin Lake area (Yukon Water Well Registry website; https://yukon.ca/en/get-information-about-yukon-groundwater-and-wells). These data provide information on: subsurface geology, depth to bedrock, and subsurface temperature. In total, the Yukon Water Well Registry contains information on 31 water wells near the Village of Teslin (Fig. 5). Most of the water wells have a geologic log. Three of these wells, located a few kilometres southeast of the Village of Teslin, hit bedrock at depths ranging from 1–12 m (rock types encountered include greywacke, siltstone, and shale). And a 182 m deep hole drilled near the middle of town in Teslin reported a depth-to-bedrock of 130 m (encountering chlorite schist). All other geology logs from the water wells reported gravel, sand, silt, and clay as the materials encountered downhole.

Subsurface temperature measurements are available in the Teslin area only from very shallow depths. Two wells in the Village of Teslin (VOT TW10-2 and Community Well 203020003) have reported subsurface temperatures of 3.5–5.2 °C at depths of 20–30 m.

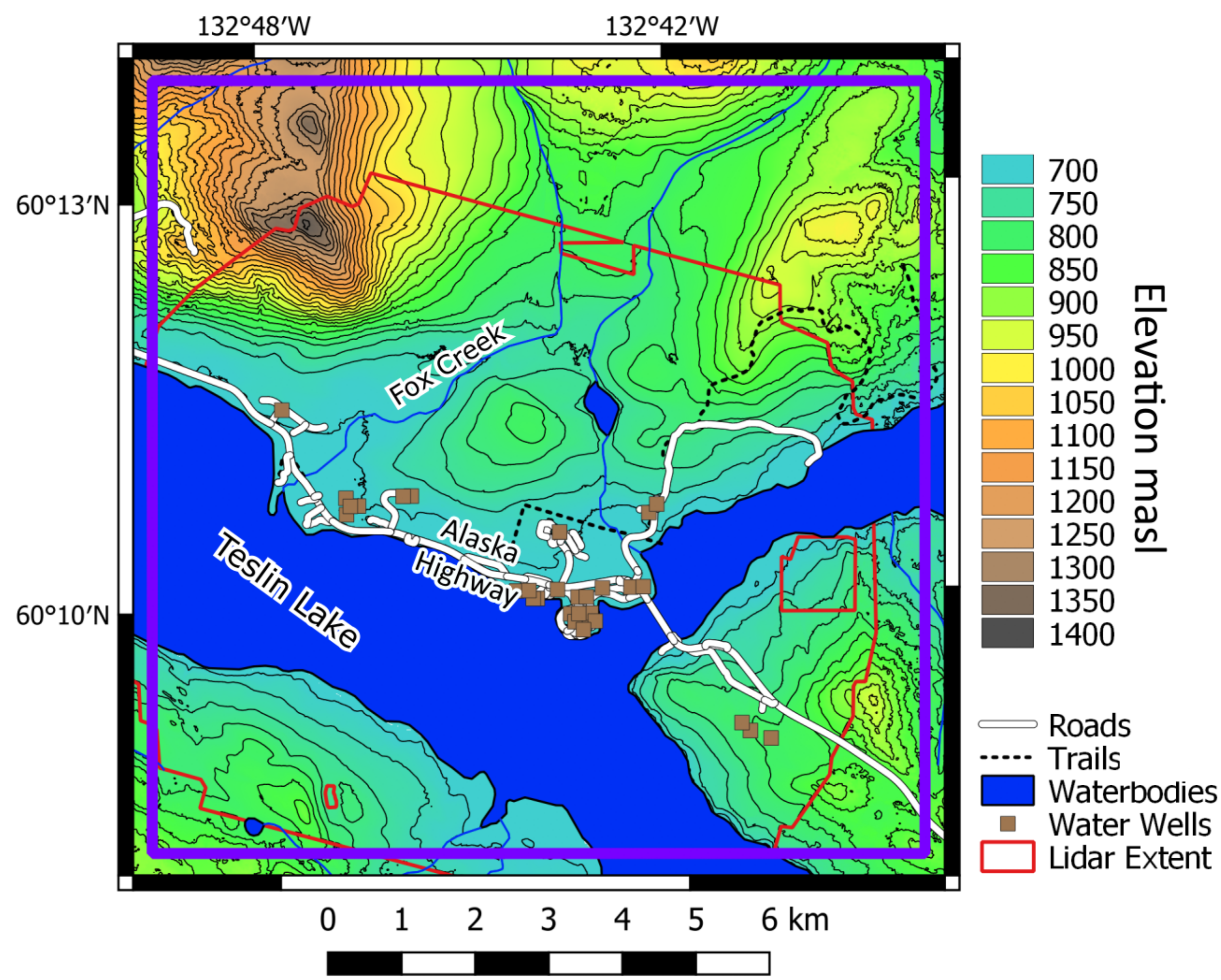

Figure 5. *Detailed topography of the study area (purple box) based upon merged LiDAR, Arctic DEM, and CDED data. Extent of LiDAR coverage shown (red polygon). Topographic contours are 25 m. Locations of water wells are also plotted (brown squares).*

Gravity survey data

Regional-scale gravity data were obtained from the NRCAN Geoscience Data Repository for Geophysical Data (http://gdr.agg.nrcan.gc.ca/). In the Teslin area, gravity measurements are generally quite sparse (~10 km station spacing). However, gravity data with a much tighter average spacing (~750 m to 2 km) have been collected along the Alaska Highway and Canol Road. When these gravity datapoints are gridded (Fig. 6), it reveals a gravity high under the Village of Teslin and another adjacent to the western strand of the Teslin fault zone, southeast of Hayes Peak. Other areas are characterized by predominantly low to moderate gravity response. Geologically, some of these gravity highs may represent buried bodies of ultramafic rocks since such lithologies outcrop locally in these portions of the Cache Creek and Quesnellia terranes. The regions of low-to-moderate gravitational response are likely a reflection of relatively lower density plutonic and meta-sedimentary rocks in the area.

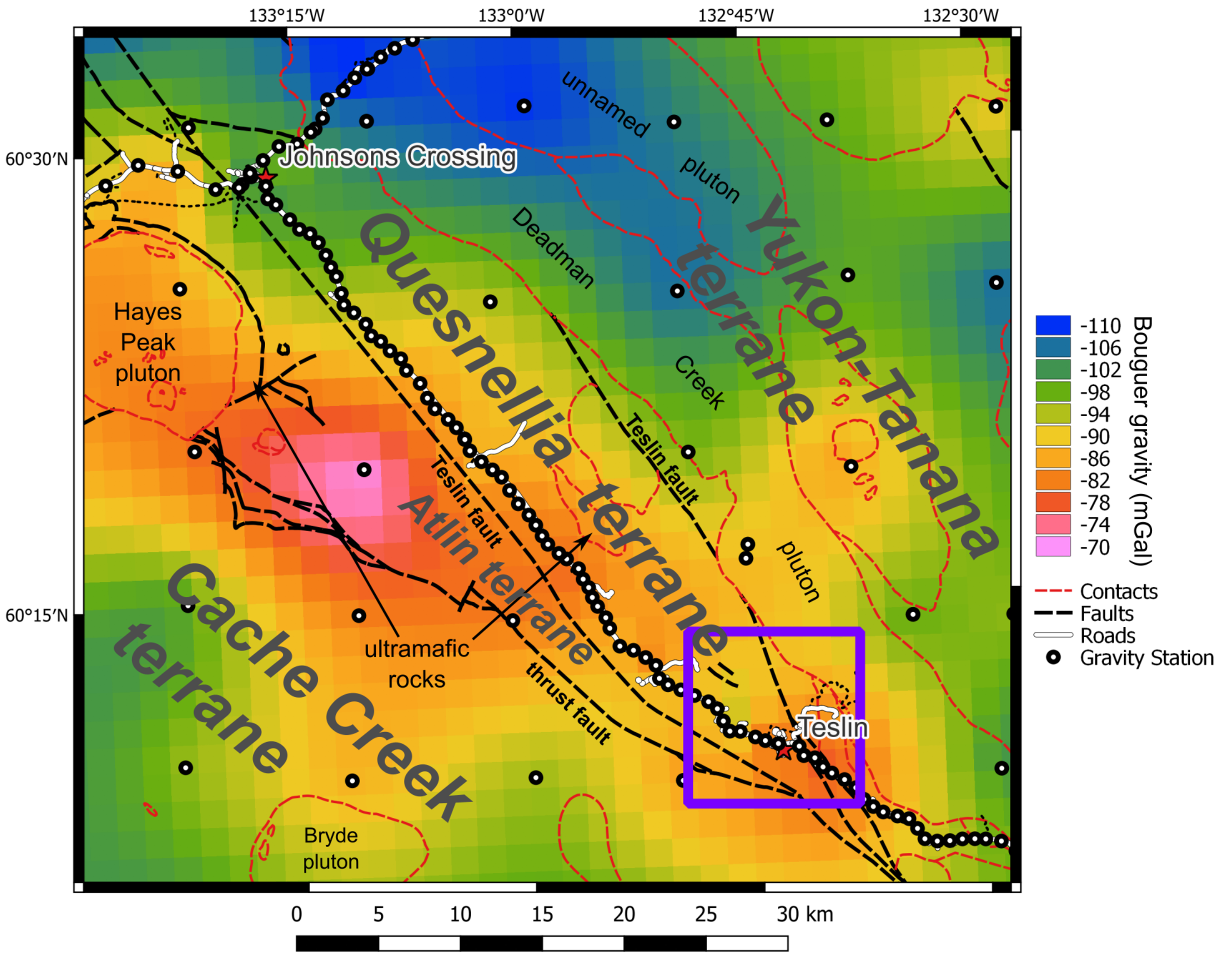

Figure 6. *Regional scale Bouguer gravity map for the Teslin area. Gridded gravity data are shown as the coloured background with cool/warm colours representing gravity lows/highs. The locations of gravity measurement points are overlain. The study area is shown by the purple rectangle.*

Airborne magnetic survey data

Magnetic survey data were obtained for the Teslin study area from the Yukon Geological Survey (Kiss and Boulanger, 2018). The YGS magnetic survey data were already gridded with a ~100 m cell size and these data were used for both the map-based interpretation and the 3D magnetic inversion modelling.

Overall, the Total Magnetic Intensity – Reduced to Pole (TMI-RTP) data generally correspond to the mapped geology (Fig. 7). For example, some mapped plutons (e.g., Bryde and north half of Deadman Creek) correspond to magnetic highs. Other plutons, however (e.g., Hayes Peak, south half of Deadman Creek, and an unnamed pluton) have moderate to low magnetic intensities. Regions where ultramafic rocks are mapped at the surface reliably correspond to magnetic highs. The strongly magnetic region immediately east of the Village of Teslin corresponds to the volcanic rocks of the Finlayson assemblage. In contrast, most of the Quesnellia terrane between the two strands of the Teslin fault has moderate to low magnetic intensity. Similarly, magnetic intensity in the Cache Creek terrane is mostly low. Structurally, a magnetic lineament is found in proximity and parallel to a portion of the southern strand of the mapped Teslin fault. These may correspond to the basalts of the Nakina Formation. There are no strong magnetic lineaments, however, that coincide with the northern strand of the Teslin fault.

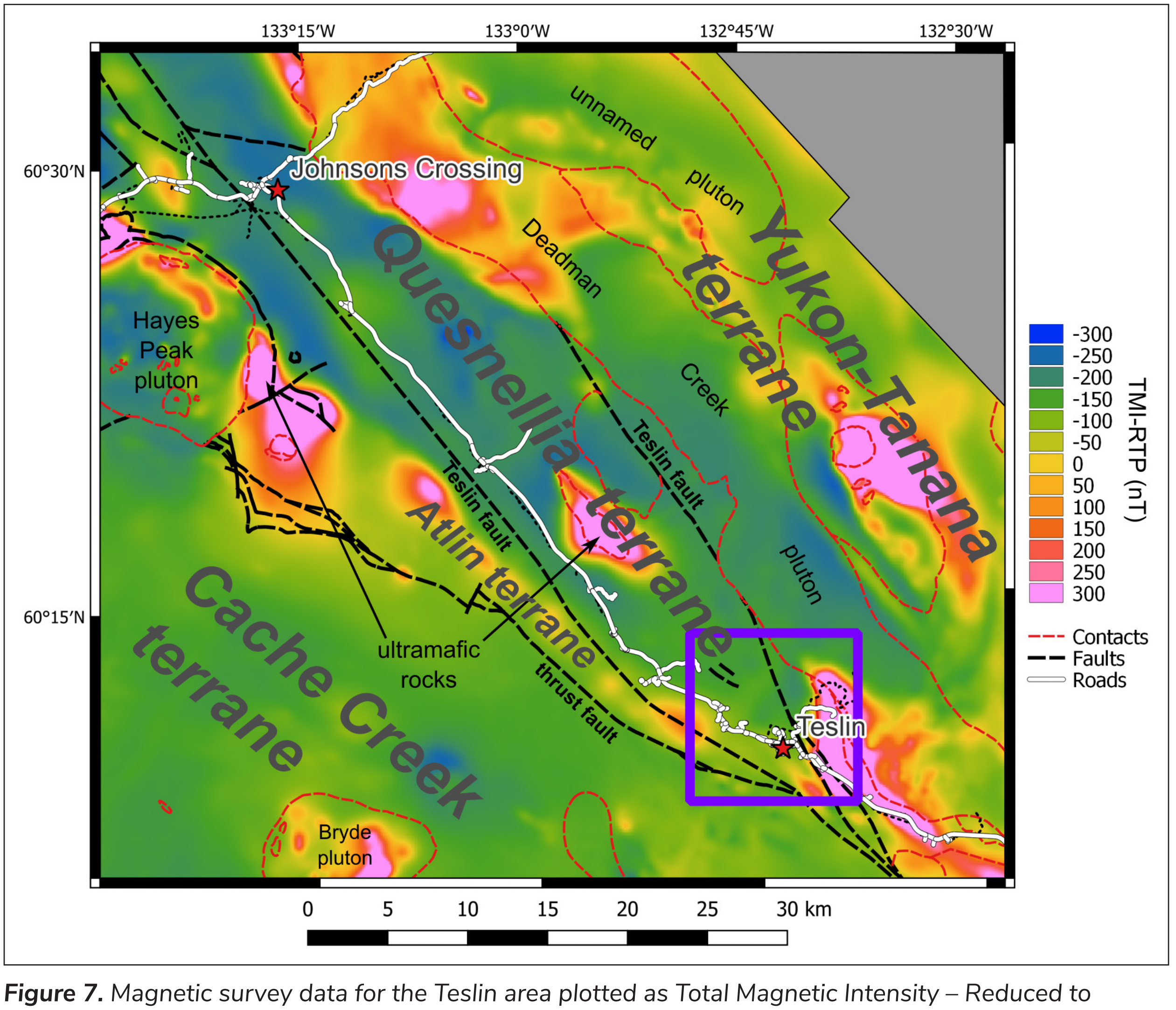

Figure 7. *Magnetic survey data for the Teslin area plotted as Total Magnetic Intensity – Reduced to Pole (TMI-RTP). The data are gridded with a 100 m cell size and coloured with cool/warm colours representing magnetic lows/highs. The study area is shown by the purple rectangle.*

Other existing geoscience data

SNORCLE 2D seismic data

Two-dimensional seismic data were collected ~40 km northwest of the Teslin study area as part of the Lithoprobe SNORCLE program. Specifically, SNORCLE Line 3 strikes approximately northeast-southwest and crosses the Teslin fault zone at Johnsons Crossing. Snyder *et al.* (2005) reprocessed SNORCLE seismic reflection data in parallel with P-wave tomographic data to generate new seismic profile interpretations for Line 3. They found northeast-dipping reflectors, down to a few kilometres' depth, between the two strands of the Teslin fault. In addition, a region of relatively lower seismic velocity also appears to coincide with the zone between the two strands of the Teslin fault. Overall, Snyder *et al.* (2005) conclude that the Teslin fault zone dips shallowly to the east and roots in the mid-crust.

SNORCLE magnetotelluric data and 2D resistivity model

As part of the Lithoprobe SNORCLE project, magnetotelluric soundings were made along the Alaska Highway from south of Teslin to past Johnsons Crossing, as well as along the Canol Road, with an average spacing of ~15 km. A portion of these MT datapoints that pass northeast-southwest through Johnsons Crossing have been modeled as a 2D resistivity profile by Dehkordi et al. (2019); the resistivity profile corresponds to SNORCLE seismic Line 3 and extends from the surface to a depth of 40 km. The subsurface resistivity variations along the profile show moderate resistivity values (*e.g.*, 500 – 1000 Ωm) associated with the Teslin fault zone and Quesnellia terrane, whereas higher resistivity rocks (~10,000 Ωm) have been mapped in the adjacent Cache Creek and Yukon-Tanana terranes. Low resistivity rocks (*e.g.*, < 10 Ωm) have not been identified in the subsurface near the Teslin fault zone. A geologic interpretation of moderate to high resistivity regions observed in the subsurface in the Dehkordi et al. (2019) study is that they are consistent with relatively unaltered, dry, and impermeable rocks lacking graphite. Note that a similar 2D resistivity profile, using MT stations along the Alaska Highway and passing through the Village of Teslin is not available.

Resource exploration assessment reports

Assessment reports from mineral exploration activity in the Teslin region were also reviewed. Overall, the information in the assessment reports were of limited assistance to improve understanding of the regional geologic framework. For example, mineral exploration holes were drilled at only two localities in the vicinity of Teslin Lake: ~5 km west of the Hayes Peak pluton (Delayee prospect) and ~12 km northwest of Johnsons Crossing (Tes prospect). Public domain drilling records for these prospects were reviewed but no downhole temperatures were reported.

Newly collected geoscience data

Gravity survey data

In 2021, a ground-based gravity survey was proposed as the next step in a geothermal exploration program for the Teslin area. Gravity data would be helpful to improve understanding of the geometry of rock units and orientation of geologic structures associated with the Teslin fault zone. Such fault structures could potentially serve as permeable pathways for the ascent of warm geothermal fluids.

A 10 km x 10 km gravity survey area containing a uniform grid of gravity stations spaced 500 m apart was proposed. The gravity survey area was co-located with the best road access (*e.g.*, Alaska Highway, side roads, and trails) and approximately centered on the Village of Teslin.

Geologically, the proposed survey area covered both strands of the Teslin fault as well as a mapped thrust fault adjacent to the south shore of Teslin Lake.

In 2022, Aurora Geosciences collected new gravity measurements from 427 stations using the proposed 500 m spacing (Fig. 8). An additional 245 gravity measurements with 100 m station spacing were collected in a ~2 km x ~3 km area covering the Village of Teslin. High-resolution GNSS (Global Navigation Satellite System) elevation measurements were also made at each gravity station. About 90 gravity stations were collected on the surface of Teslin Lake when the lake was frozen. To properly correct for the presence of the low-density body of lake water, Aurora Geosciences also conducted a boat-based bathymetric survey of Teslin Lake within the study area along survey lines spaced ~250 m apart. The overall measurement error for the 2022 gravity survey is estimated at 0.061 mGal. A full description of the gravity and bathymetry data acquisition by Aurora Geosciences is in Appendix 3.

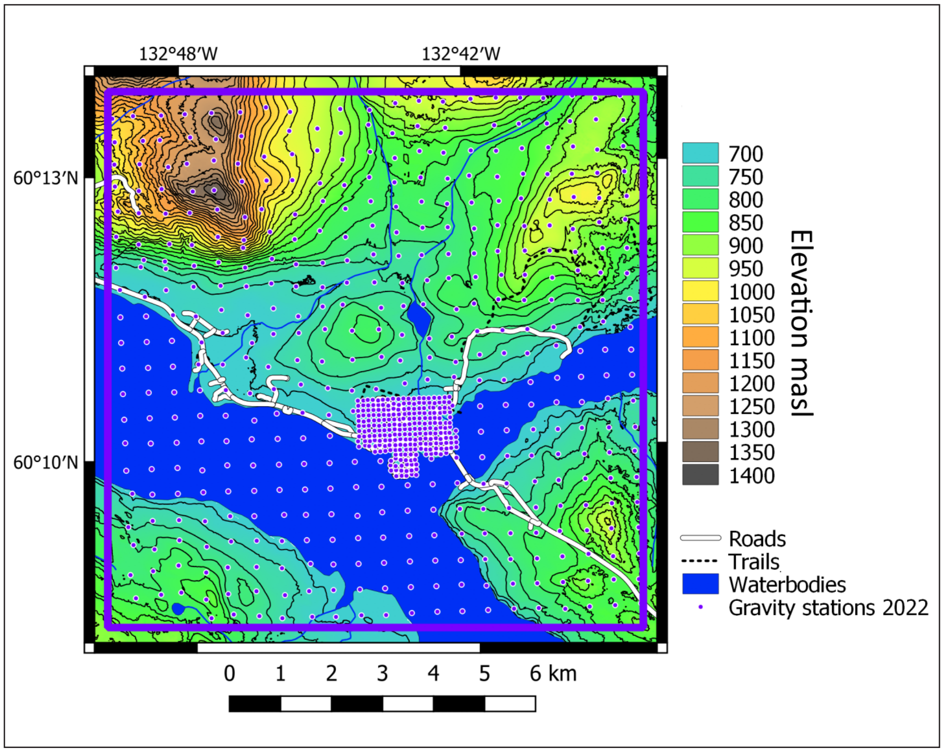

Figure 8. *Map showing gravity stations (purple dots) occupied in the 2022 gravity survey by Aurora Geosciences. The survey area is ~10 km x ~10 km (purple rectangle). The background image shows topography, water bodies, and road/trail access.*

Audio-magnetotelluric survey data

As part of this project, Geological Survey of Canada (GSC) researchers conducted a reconnaissance audio-magnetotelluric (AMT) survey in the study area to better understand subsurface electrical resistivity variations on a broad scale. A total of 7 AMT stations were occupied across the central portion of the study area from southeast to northwest (Fig. 9). The AMT survey employed a frequency range of 8000 Hz to 5 Hz.

Rock property data

There are few opportunities to sample bedrock for rock properties (e.g., rock density and magnetic susceptibility) given limited outcrops in the Teslin area. Nonetheless, YGS personnel visited the greater Teslin area in 2021 and collected 33 hand samples for rock property analysis that are representative of the following rock units: Deadman Creek pluton (n=1), Cache Creek terrane (n=2), Nakina Formation (n=2), Snowcap assemblage (n=8), Shonektaw Formation (n=15), and the Finlayson assemblage (n=5). The samples do not all come from within the boundary of the

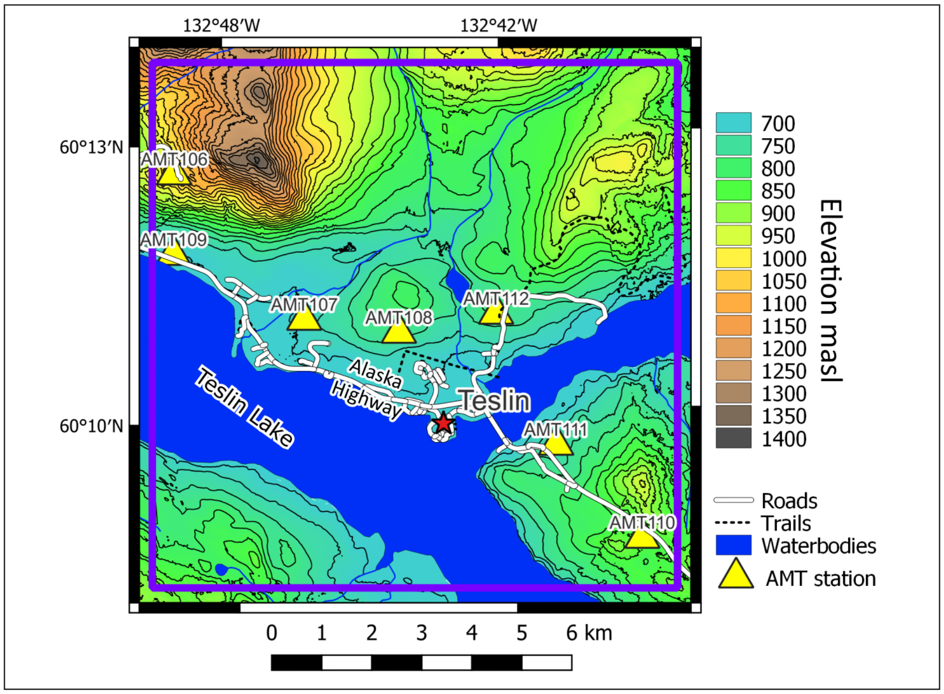

Figure 9. *Map showing AMT station locations (yellow triangles) occupied in the 2022 AMT survey by the Geological Survey of Canada.*

study area, but they do come from mapped rock units that represent all of the six major rock types present within the study area. Magnetic susceptibility was measured on outcrop and hand samples in the field, while density was measured on hand samples in the Yukon Geological Survey laboratory in Whitehorse. Additional, rock property data for the Deadman Creek pluton (n=4) were obtained from Colpron et al. (2021). Rock property data for near surface sediments are not available so representative values were estimated.

Methodology

Map-based interpretation

To better characterize the structural and geologic framework within the study area, the following data sets were interpreted using a map-based approach: topography, gravity, magnetics, and geology. All map-based interpretation was performed with the software QGIS (qgis.org).

Various filters were applied to the gravity and magnetic survey data to aid map-based interpretation of the spatial extent of dense and magnetic rock units as well as the orientation of inferred fault structures that lie under sedimentary cover. These filters include: first vertical derivative, total horizontal gradient, and tilt derivative, as well as analytic signal (magnetics only). Geophysical filtering was performed using Geoscience Analyst Pro software (https://mirageoscience.com/). The gravity and magnetic geophysical data were interpreted in conjunction with the mapped geology (e.g., Colpron, 2022) and rock properties to better understand the geophysical response of the major rock units in the study area.

3D geology modelling

3D geologic models were constructed for the study area to aid in interpretation and to serve as an important constraint for 3D gravity inversion modelling. Rhinoceros software (www.rhino3d.com) was used to build the 3D geologic model as surfaces that represent geologic horizons and faults. The 3D geologic model was built to honour the bedrock geology map of Colpron (2022) as much as possible.

3D gravity modelling

3D geophysical inversion modelling of gravity data was performed as part of the effort to iteratively build a 3D geologic framework for the project area. Gravity data are sensitive to changes in subsurface rock density and rock density can be used as a proxy for rock type, provided sufficient density contrasts between rock units are present. The 3D inversion modelling of gravity data pursued here was guided by both the 3D geologic model described above as well as average rock density values for each geologic unit. The inversion algorithm employed for the modelling is the open source SimPEG code (Cockett *et al.*, 2015). We used both rock property and geologically constrained inversion strategies as described by Fullagar and Pears (2007) and Fullagar *et al.* (2008). In addition, we used spatially variable mixed Lp norms for the model regularization as described in Fournier and Oldenburg (2019).

The 3D gravity model volume has the following dimensions 10.5 km east-west x 10.5 km north-south x 4.5 km thick. We assumed a background rock density value of 2.67 g/cm^3. The 3D model mesh consists of cubic cells of the following sizes: 50 m cells from 0–500 m depth, 100 m cells from 500–2500 m depth, and 200 m cells from 2500–4000 m depth. Two kilometres of padding cells were added to the model volume on the sides and bottom to minimize edge effects. The topographic surface utilized for the 3D geophysical model volume was stitched together from LiDAR, Arctic DEM, and CDED data (Appendix 3). A total of 671 gravity data points were used in the inversion modelling. The gravity data consisted of Complete Bouguer Anomaly gravity values with a terrain correction density of 2.67 g/cm^3. The gravity data were upward continued by 500 m prior to inversion modelling to minimize near surface effects and model artifacts.

3D magnetic modelling

Magnetic data are sensitive to variations in the magnetic susceptibility of rocks in the subsurface. Due to the presence of the magnetic high anomaly spatially associated with the Finlayson assemblage, 3D geophysical inversion modelling of magnetic data was primarily performed to help better estimate the depth and geometry of that rock unit.

Like the 3D gravity modelling, the 3D inversion modelling of magnetic data was also guided by a 3D geologic model and average magnetic susceptibility values for each rock unit. The magnetic inversion modelling used the open source SimPEG code (Cockett *et al.*, 2015) and spatially variable mixed Lp norms for the regularization (Fournier and Oldenburg, 2019). The 3D magnetic model volume is the same size as the one used for the 3D gravity modelling. Similarly, the model mesh and cell sizes are also the same. Two kilometres of padding cells were added to the model volume on the sides and bottom to minimize edge effects.

A total of 10 815 magnetic survey data points were used in the inversion modelling, derived from gridded TMI magnetic survey data from Kiss and Boulanger (2018). Magnetic field parameters used for the inversion modelling include declination (19.988°), inclination (76.185°), and total field strength (56 707.8 nT). Lastly, for simplicity, we assumed that remanent magnetization of rocks is not present in the project area.

Limitations and uncertainty of 3D geophysical inversion modelling

For all geophysical models, non-uniqueness is a problem such that even if a geophysical model is mathematically correct and matches the surface geophysical measurements quite well, it may not necessarily be geologically correct. In this study, we try to reduce this uncertainty by attempting to simultaneously match the geophysical measurements, rock property data, and a geologically reasonable 3D geology model that honours bedrock geology mapping.

Results

Map-based interpretation

Gravity survey data

Complete Bouguer Anomaly (CBA) gravity data collected for this study, with a terrain correction density of 2.67 g/cm^3, has the range -96 to -78 mGal (Fig. 10). The key features of the gravity map include:

- a gravity low in the northeast corner that coincides with the Deadman Creek pluton;
- a northwest-trending trough of low gravity that approximately coincides with Teslin Lake;
- a large area of elevated gravity response that generally corresponds to the Shonektaw and Snowcap rock units;
- a pronounced, northeast-trending trough of low gravity located in the northwest quadrant of the study area that approximately coincides with Fox Creek (see Figure 5 for location of Fox Creek); and
- a second, but much more subtle, northeast-trending trough in the gravity (lower relative to its surroundings) in the southeast quadrant of the study area that coincides with the Nisutlin Arm of Teslin Lake.

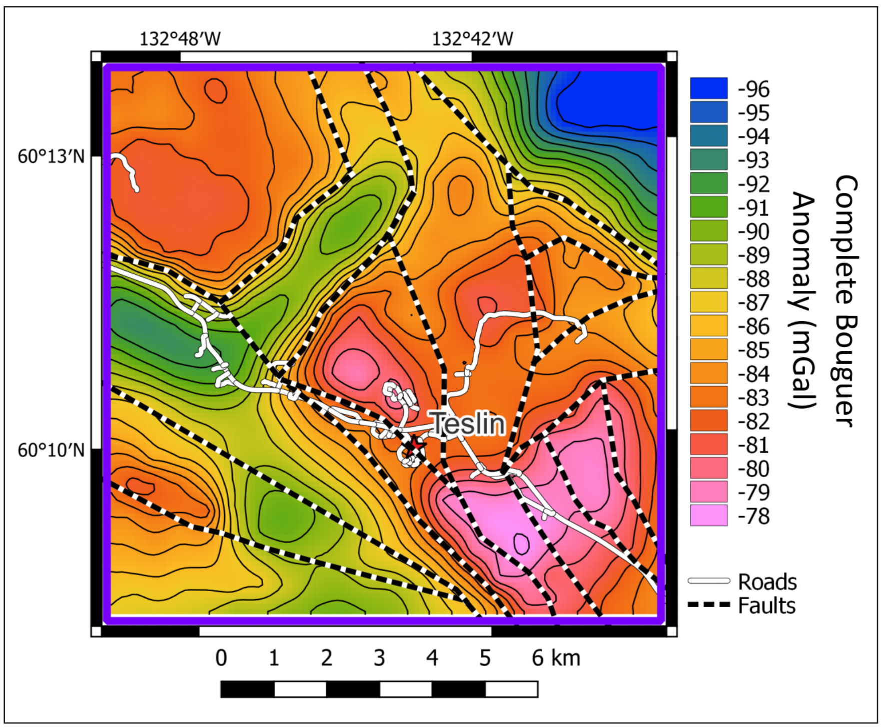

Figure. 10. *Complete Bouguer Anomaly (CBA) gravity data gridded with a 100 m cell size. Gravity contours (black solid lines) are shown at 1 mGal intervals. Black and white dashed lines are faults inferred from both the gravity and magnetic survey data (See Figures 12 and 13).*

The northwest-trending trough of low gravity and the subtle northeast-trending trough of low gravity, mentioned above, both reflect the influence of low-density water from Teslin Lake on the gravity response. In this study, northwest and northeast-trending fault structures near the lake have been inferred from the gravity; however, confidence in these faults is low based upon gravity interpretation alone. Corroborating evidence for faults co-located with margins of Teslin Lake would be helpful. Of greater interest, however, is the pronounced northeast-trending trough of low gravity near Fox Creek, where there is no lake water to generate the low gravity.

Instead, a thick section of low-density sediments would be the most likely explanation of the gravity low near Fox Creek and raises the question of how a thick layer of sediments could be present there. Options include: 1) a sediment-filled trough carved out by glaciers; 2) a sediment-filled trough generated via extensional tectonics along normal faults within the Teslin fault zone; or 3) some combination of the two.

A total horizontal gradient (THG) filter was applied to the gravity data to highlight the zones of greatest horizontal change in the gravity (Fig. 11). Total horizontal gradient maps are commonly used in gravity interpretation to infer fault or rock unit contacts since THG high anomalies represent zones of strong density contrast. The THG gravity map generated for the study area clearly shows the boundaries of the northeast-trending trough near Fox Creek. The THG gravity map also shows a strong, northwest-trending density contrast located south of the Village of Teslin. Both areas likely represent important, fault-bounded contacts. Most of the rest of the THG gravity map shows areas with much more subtle THG anomalies that are challenging to tie directly to the surface geology.

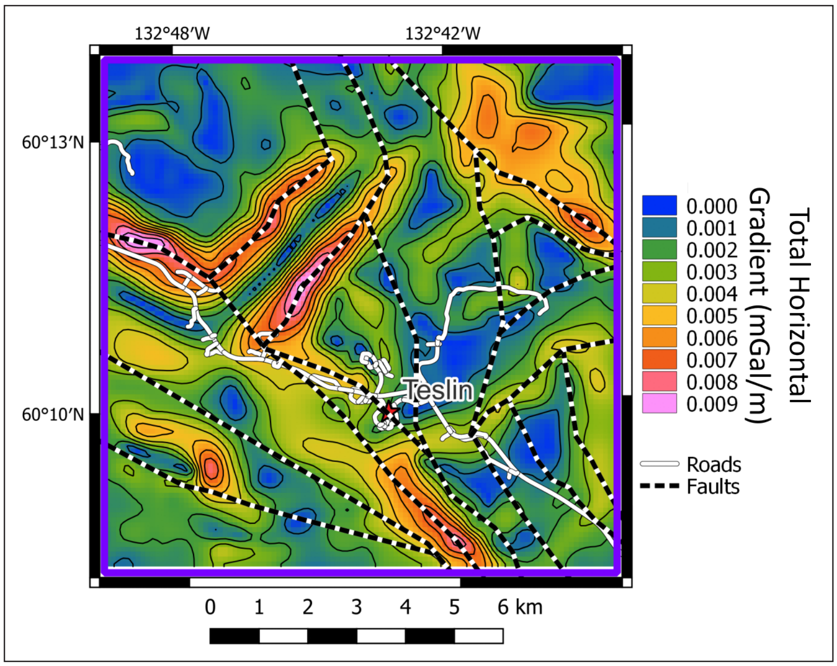

Figure. 11. *Complete Bouguer Anomaly gravity data upward continued by 100 m and with the total horizontal gradient (THG) filter applied. Black and white dashed lines are faults inferred from both the gravity and magnetic survey data (See Figures 12 and 13).*

Magnetic survey data

Within the study area, the Total Magnetic Intensity (TMI) map with Reduction to Pole (RTP) applied has the range -195 nT to +1153 nT (Fig. 12). The key features of the magnetic map include:

- a strong magnetic high in the east and southeast that coincides with the Finlayson assemblage;
- a low magnetic response in the northeast corner corresponding to the Deadman Creek pluton;
- a low-magnitude, northwest-trending magnetic high that approximately corresponds to Teslin Lake;
- a very subtle, northeast-trending magnetic signature that matches the gravity trough found near Fox Creek; and
- generally low magnetic response in other areas that correspond to the Shonektaw and Snowcap rock units.

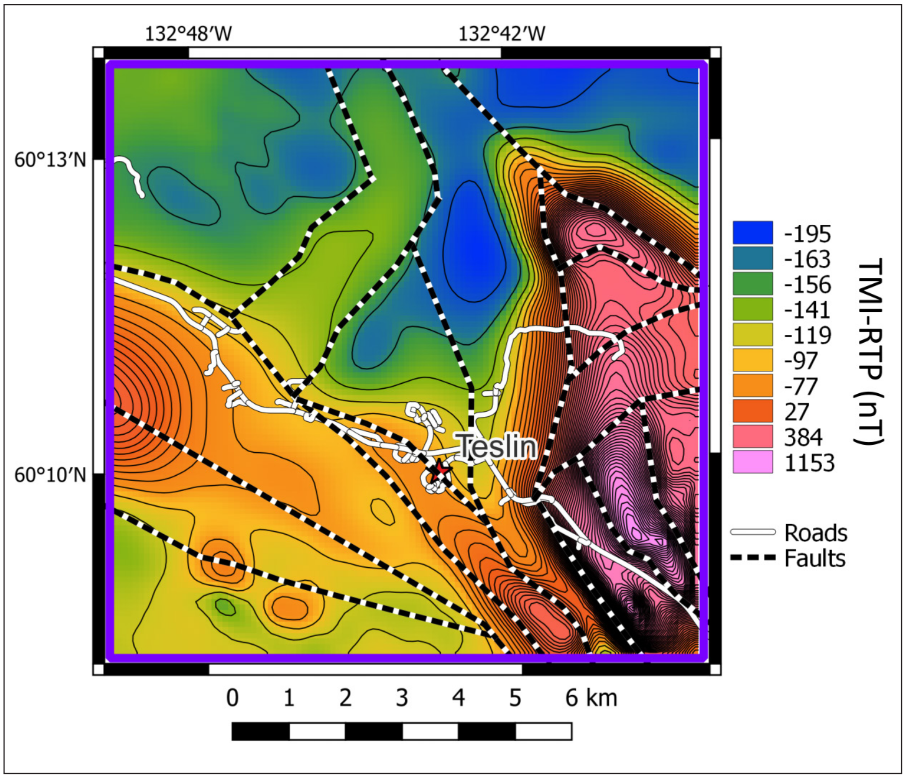

Figure 12. *Magnetic survey data gridded with a 100 m cell size clipped to the Teslin study area (Kiss and Boulanger, 2018). Total Magnetic Intensity with Reduction to Pole applied (TMI-RTP) is shown here. Black and white dashed lines are faults inferred from both the gravity and magnetic survey data (See Figures 10 and 11).*

The broad magnetic high associated with Teslin Lake likely indicates that sediments on the floor of the lake contain magnetic minerals and were transported to the lake, by fluvial or glacial action, from a magnetic terrane located elsewhere. Similarly, the subtle northeast-trending magnetic signature could also indicate a layer of magnetic sediments filling the Fox Creek valley.

A total horizontal gradient (THG) filter was also applied to the magnetic data to highlight the zones of greatest horizontal change in the magnetic response (Fig. 13). The THG magnetic map marks many linear features of strong gradient within the highly magnetic Finlayson assemblage (east and southeast portions of the study area) that have been interpreted here as faults both within and bounding the Finlayson assemblage.

Rock property data analysis

The rock property data collected for this study were categorized according to the major rock unit to which they belong and were graphed as box and whisker plots for better visualization of the data distribution (Fig. 14). Simple statistics (*i.e.*, maximum, minimum, mean and 1σ standard deviation) were calculated to assess the variation in the results (Table 1). The average rock property values shown in Table 1 are assumed to be representative of each rock unit and, therefore, were used as starting and reference values in the 3D geophysical inversion modelling.

As shown in Figure 14, average rock density is generally low for the Deadman Creek pluton (2640–2710 kg/m^3) as well as for the Cache Creek terrane (2660 kg/m^3). The Snowcap assemblage contains two lithologies with distinctly different densities: a quartzite lithology (2640 kg/m^3) and one described as conglomerate or schist (*i.e.*, not quartzite; 2760 kg/m^3). The Shonektaw and Finlayson rock units also have a variable but high average density (2840 and 2790 kg/m^3, respectively) and, finally, the Nakina Formation has the highest density (2980 kg/m^3) of all the rocks in the study area.

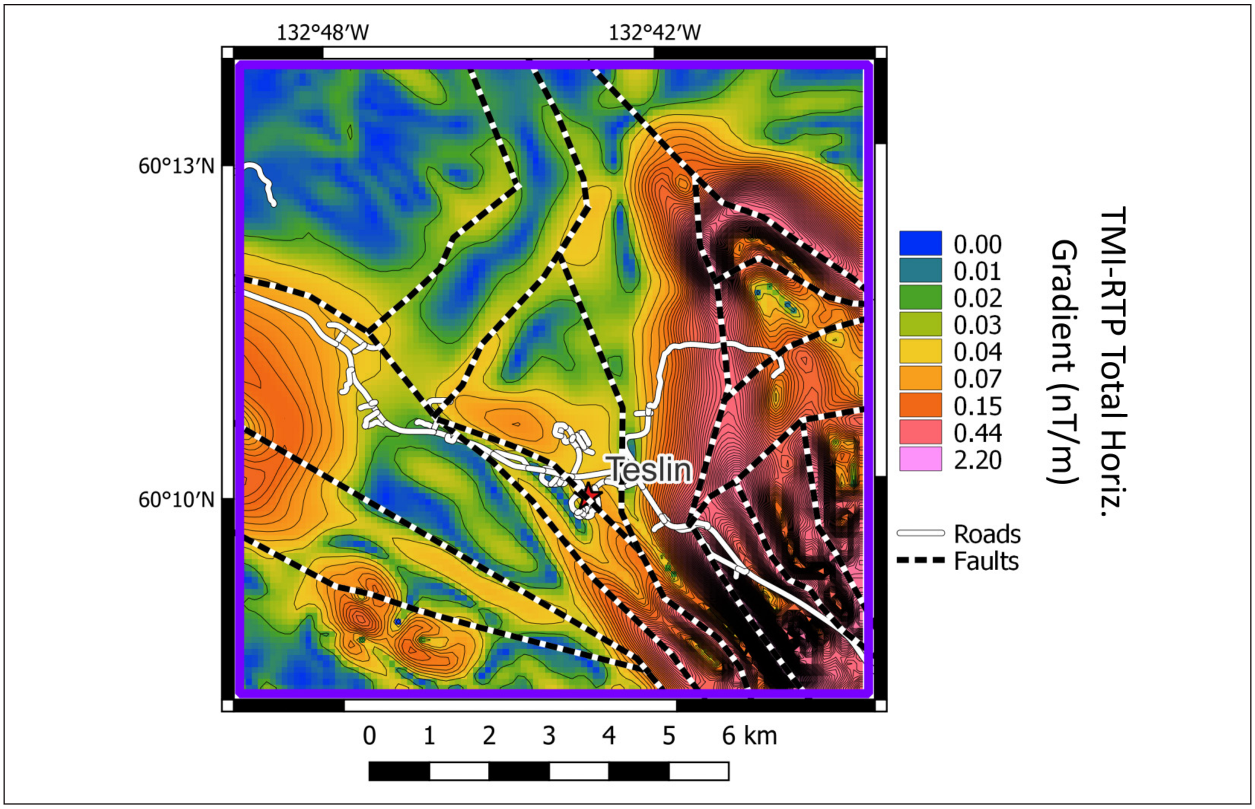

Figure 13. *Magnetic survey data gridded with a 100 m cell size clipped to the Teslin study area (Kiss and Boulanger, 2018). Total Magnetic Intensity with Reduction to Pole (TMI-RTP) and the Total Horizontal Gradient filter is shown here. Black and white dashed lines are faults inferred from both the gravity and magnetic survey data (See Figures 10 and 11).*

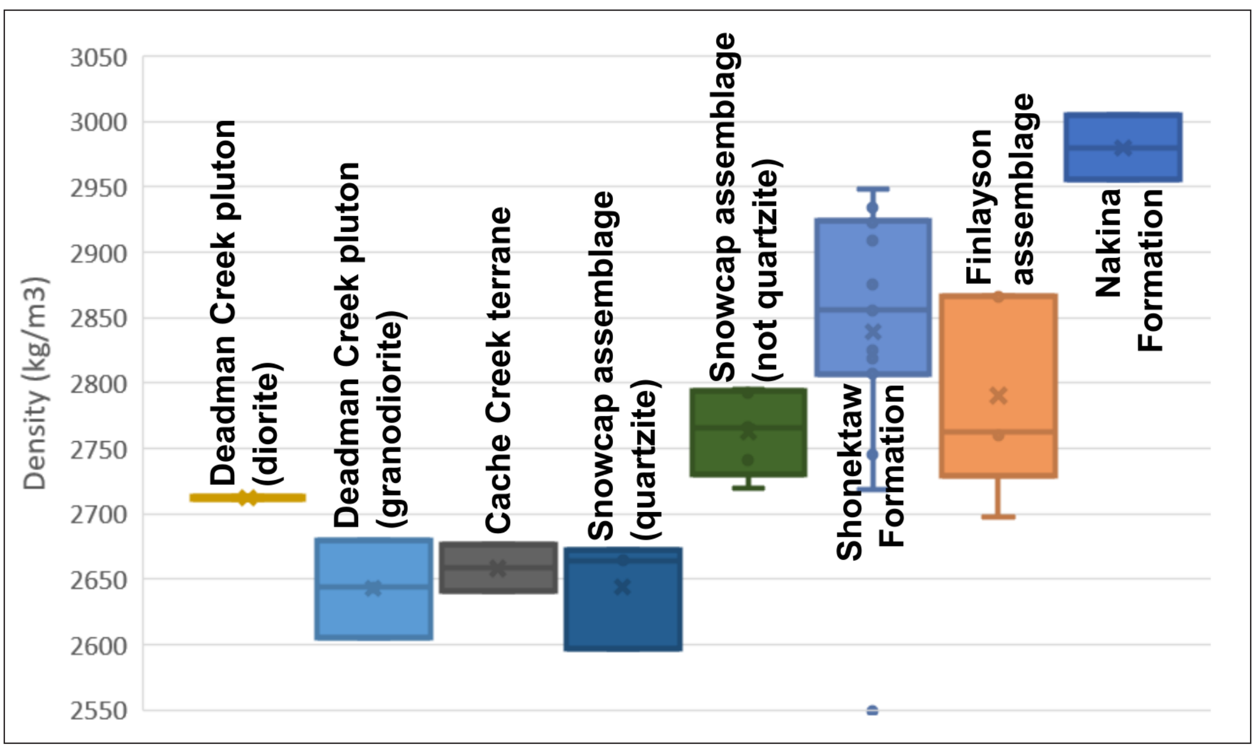

Figure 14. *Rock density data compiled from 37 hand samples that are representative of rock units in the study area.*

As shown in Figure 15, average magnetic susceptibility is very low for the Deadman Creek pluton, Cache Creek terrane, and quartzite lithology of the Snowcap assemblage (< 0.0002 SI). These rock units are essentially magnetically indistinguishable from one another. The Shonektaw and Nakina rock units have average magnetic susceptibility values that are only slightly higher (~0.0007 SI). In contrast, the non-quartzite Snowcap lithologies and the Finlayson assemblage are both strongly magnetic (0.026–0.028 SI) and have a rather wide range in magnetic susceptibility. Rock property data for near surface sediments (either glacial or lake sediments) were not available for this study and, thus, we use assumed values (Table 1).

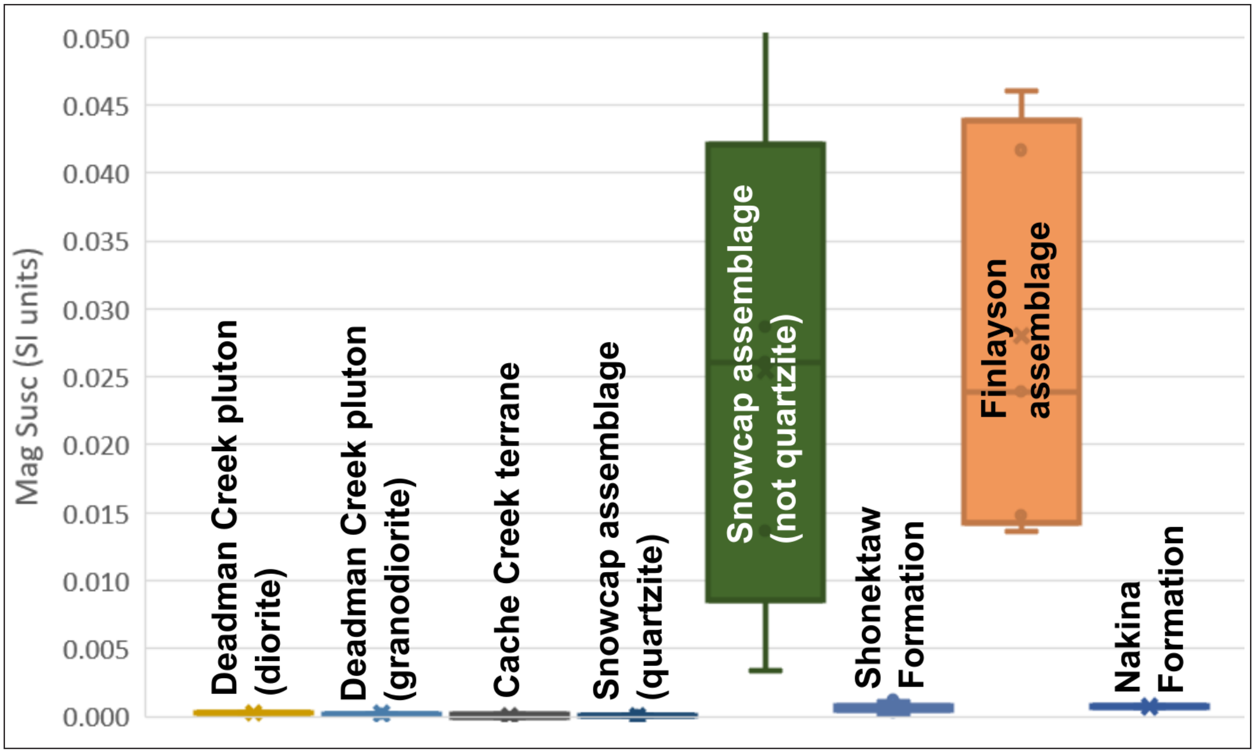

Figure 15. *Rock magnetic susceptibility data compiled from 37 hand samples that are representative of rock units in the study area.*

Integrated 3D geoscience model interpretation

Interpretation of the audio-magnetotelluric (AMT) resistivity model

A key unknown at the start of this project was the variation in thickness of the near surface sediments in the Teslin area (*i.e.*, both glacial sediments and lake sediments). This is important because variations in sediment thickness can have a strong influence on the gravity and magnetic model results. Sparse, existing data suggests that the sediment thickness has a minimum range of 0 m (bedrock exposed at the surface) to 130 m (measured in the deepest water well in the Village of Teslin). For most of the study area, however, there is no information on the depth-to-bedrock. Thus, an AMT resistivity model might be able to help us identify, in a broad sense, regions of the study area where thick sections of sediments are more likely and other areas where sediment cover is thin or absent. We assume that near surface sediments in the study area are characterized by lower resistivity (*i.e.*, < 20 ohm.m) due to their clay content, which contrasts with more resistive bedrock units.

A preliminary 3D resistivity model of the AMT data, generated by the Geological Survey of Canada (V. Tschirhart, 2023, personal communication) was made available for this study.

Table 1. Simple statistics of the A) density data and B) magnetic susceptibility data categorized according to rock type. n = number of measurements. Rock property values for near surface sediments are assumed.

A) Rock density data

Rock unit	Minimum (kg/m³)	Maximum (kg/m³)	Average (kg/m³)	1σ Std. Dev. (kg/m³)	n
Deadman Creek (diorite)	2711	2713	2712	1	2
Deadman Creek (granodiorite)	2605	2680	2643	38	3
Cache Creek terrane	2640	2676	2658	25	2
Snowcap assemblage (quartzite)	2596	2672	2644	42	3
Snowcap assemblage (not quartzite)	2720	2794	2763	32	5
Shonektaw Formation	2549	2948	2839	107	15
Finlayson assemblage	2697	2866	2790	74	5
Nakina Formation	2955	3004	2980	35	2
Near surface sediments	n/a	n/a	2200	n/a	0

B) Rock magnetic susceptibility data

Rock unit	Minimum (SI units)	Maximum (SI units)	Average (SI units)	1σ Std. Dev. (SI units)	n
Deadman Creek (diorite)	n/a	n/a	0.000240	n/a	1
Deadman Creek (granodiorite)	0.000199	0.000200	0.000200	0.000003	3
Cache Creek terrane	0.000004	0.000113	0.000059	0.000077	2
Snowcap assemblage (quartzite)	0.000029	0.000097	0.000060	0.000034	3
Snowcap assemblage (not quartzite)	0.003410	0.055500	0.025482	0.019607	5
Shonektaw Formation	0.000169	0.001290	0.000615	0.000282	15
Finlayson assemblage	0.013600	0.046000	0.028000	0.015084	5
Nakina Formation	0.000669	0.000831	0.000750	0.000115	2
Near surface sediments	n/a	n/a	0.010000	n/a	0

The 3D resistivity model is interpreted here as follows. In the southeast portion of the study area, the Finlayson and Snowcap assemblages are highly resistive (>1000 ohm.m) and are mostly covered by a thin layer (*i.e.*, tens of metres or less) of low resistivity sediments. In contrast, in the northwestern part of the study area, the Shonektaw Formation likely has an intermediate resistivity (100–1000 ohm.m) and may be covered by thicker sections of low resistivity sediments (*i.e.*, more than tens of metres) in two areas: Teslin Lake and the Fox Creek valley. There is no AMT station coverage in the northeast and southwest parts of the study area, thus resistivity model results for rock units in these areas are not available.

This interpretation of the preliminary AMT resistivity model result suggests the following:

- Teslin Lake is a topographic low and a significant depositional centre so accumulation of clay-rich, low resistivity sediments there would be expected; and
- evidence for a substantial accumulation of low resistivity sediments in the Fox Creek valley is consistent with the interpretation of the gravity and magnetic data which suggests a northeast-southwest trending, sediment filled trough in that area.

3D geology + gravity + magnetic modelling

For this project, a 3D geologic model was constructed to provide a framework to help better interpret regions of potential geothermal favourability in the Teslin area (Fig. 16). A key aim of the 3D geologic model building exercise is to build a geologic volume consisting of fault planes and discrete blocks of rock that is, as much as possible, consistent with all the available geoscience data. To do this, the model was built in a multi-step manner. The very first step was to run geologically unconstrained, inversion models of the gravity and magnetic data to gain an understanding of the locations and sizes of expected highs and lows of density and magnetic susceptibility without the influence of any imposed geology. Unconstrained geophysical models never perfectly match the subsurface geology, but they are useful to give a preview of what to anticipate. The next step is to build a simple geologic model that consists of only two rock units (low density sediments and high-density bedrock). In the third (and most important) step, different bedrock units and geologic details are added sequentially, then 3D gravity and magnetic inversion modelling is performed multiple times to test whether each of the geologic modifications honours the geophysical datasets.

For each 3D gravity inversion, different rock units in the 3D geologic model were assigned reference density values based upon rock density measurements. Similarly, for each 3D magnetic inversion, the rock units in the 3D geologic model were assigned reference magnetic susceptibility values based upon rock property measurements (Table 1). In the inversion calculations, the inversion algorithm adjusted the rock property values (either density or magnetic susceptibility) in the model cells until a match was achieved with the measured geophysical data (*i.e.*, either gravity or magnetic survey data). For the gravity modelling, a match was achieved when the root-mean-squared (RMS) misfit, calculated for the 3D density model, reached the average measurement error of the gravity survey data (*i.e.*, 0.061 mGal). The actual calculated RMS misfit obtained for the final 3D density model is 0.051 mGal. Similarly, the estimated error on the magnetic survey data is ~5 nT; we used this value as the target misfit during the magnetic inversion modelling. The 3D magnetic susceptibility model that was generated during the inversion modelling achieved an actual RMS misfit of 5.4 nT. Thus, both the gravity and magnetic inversion modelling exercises reached the target misfit values and the model outputs are consistent with the geophysical survey data.

The final 3D geologic model (Fig. 16) contains seven different rock units (Table 2) and largely honours the bedrock and fault mapping of Colpron (2022). The fault locations in Colpron (2022) have been moved only slightly to better the geophysical data. The major differences are that the present work contains additional faults within the major rock units to reflect the gravity and magnetic interpretation.

Many assumptions went into the creation of the 3D geologic model. For example, we assume that the rock properties for all the near surface sediments have, on average, a density of 2200 kg/m^3 and a magnetic susceptibility of 0.01 SI. These values are likely not correct since we would expect lake sediments and glacial sediments (which are lumped together here) to have different rock properties. However, in the absence of rock property measurements for the near surface sediments, these estimates suffice for the geophysical modelling performed here. We also assume that other rock units have a generally uniform density and magnetic susceptibility (*i.e.*, no significant variations laterally or vertically within a single rock unit). Normal faults inferred in the Teslin area are assumed to have typical dip angles of ~60–70 degrees, whereas strike-slip faults are assumed to be mostly vertical. Due to these many assumptions and the uncertainty associated with them, the 3D geologic model is not intended to be a 100% accurate depiction of the subsurface. Rather, the 3D geologic model is meant to be as close to reality as possible;

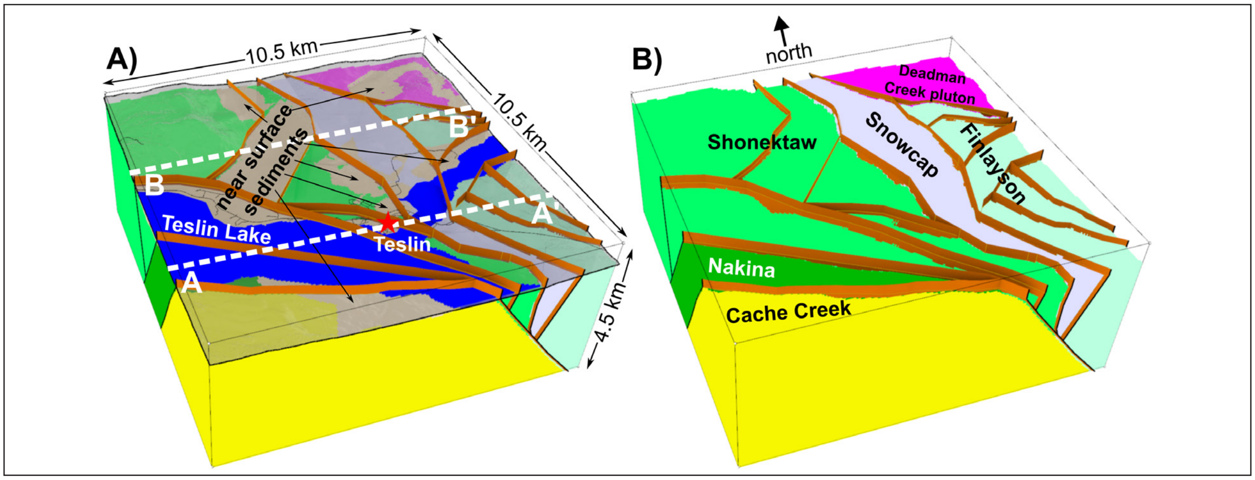

Figure 16. *Perspective view of the 3D geology model for the Teslin area.* ***A)*** *3D geology model overlain with near surface sediments (beige), lake (blue), and topography (translucent grey).* ***B)*** *3D geology model with sediments and lake removed to show bedrock units. Geologic structures are shown in brown and extend above topography to aid visualization. Dashed white lines in (A) show the locations of 2D cross-sections A-A' and B-B' extracted from the 3D model shown in Figures 17 – 22.*

Table 2. *List of rock units in the Teslin 3D geologic model.*

Rock unit name	Age	Rock type
Near surface sediments	Quaternary?	Lake sediments and glacial sediments
Deadman Creek pluton	Early Cretaceous	Granitic rocks
Cache Creek terrane	Mesozoic	Chert and shale
Shonektaw Formation	Mesozoic	Volcanic rocks
Nakina Formation	Mesozoic	Basalt
Finlayson assemblage	Paleozoic	Meta-volcanic rocks
Snowcap assemblage	Neoproterozoic & Paleozoic	Quartzite and minor greenstone

an initial 3D geologic framework which can be subsequently tested and improved with additional geophysical data and/or drilling.

The overall outcome of the 3D geology + gravity + magnetic inversion modelling effort includes new 3D rock density and 3D magnetic susceptibility models with faulted and stratigraphic geologic boundaries. Two cross-sections have been extracted from the 3D rock property models that run along east-west profiles (Figs. 17–22). Although the rock property models are in three dimensions, the 2D cross-sections presented here do highlight many of the key structural and stratigraphic elements of the rock property models.

The 2D cross-sections showing density model results (Figs. 17–18 and 20–21) contain the following elements: a reference geologic model (showing rock types), an unconstrained density inversion model output (not influenced by geologic constraints for comparison with the geologically-constrained result), a reference density model (showing the values and geometry of the geologic constraints), and a geologically-constrained density inversion model output (our best attempt to reconcile geology, gravity data, and rock property measurements). The density model results are presented using two colour scales (2000–2900 kg/m^3 and 2400–3000 kg/m^3) to help better visualize the lower density and higher density rock distribution in the density models. The 2D cross-sections showing magnetic susceptibility model results (Figs. 19 and 22) contain similar elements. However, the susceptibility model results are visualized using a log colour scale with the range 0.0001–0.1 SI units.

By comparing the density and magnetic susceptibility model results with their reference rock property and geology models we can gain insight into how good the match is between our conceptual understanding of the subsurface geology and reality. In some areas, the agreement between the reference and inversion rock property models is good. In other areas, regions of mismatch are clear and represent areas where the geologic understanding is poor, and more information is needed to help better understand the subsurface.

Explanation of cross-section A-A': through the Village of Teslin

The east-west cross-section through the Village of Teslin contains six out of the seven rock units found in the study area and many inferred faults (Fig. 17A). Key features of the geologic model in this area include: 1) east-dipping faults bounding the Nakina rock unit; and 2) a steeply west-dipping wedge of Snowcap assemblage sandwiched between the Finlayson assemblage and the Shonektaw Formation. In addition, some sediments are present on the floor of Teslin Lake but they are very thin elsewhere.

The unconstrained density inversion model (Fig. 17B) shows elevated density mainly in the vicinity of the Finlayson and Nakina rock units which is consistent with rock density measurements. Curiously, for the Shonektaw rock unit the unconstrained density model also shows a small area of high density in the shallow subsurface (under Teslin Lake, just west of the Village of Teslin) which is surrounded by moderate density material. This is curious because our expectation is that the Shonektaw unit is all high-density rock material.

The geologically constrained density inversion model results for cross-section A-A' (Fig. 17 C and D) show a good match between the reference and inversion results for the sediments, Snowcap, and Cache Creek rock units. Viewing the density inversion model results with a different colour scheme (Fig. 18 B and C) also shows a good match for the Nakina, Shonektaw, and Finlayson rock units with the exception of a handful of areas where the inversion model density is either too high or too low (marked by "??" in Figure 18C). Clearly, the geology in the areas of mismatch is more complicated than shown. One possible explanation for the abnormally high inversion model density observed in the Shonektaw unit is the presence of a dense body of ultramafic rocks (e.g., dunite, pyroxenite) like those outcropping at the surface within the Quesnellia terrane ~20 km northwest of Teslin (Fig. 3).

The unconstrained magnetic susceptibility inversion model for cross-section A-A' (Fig. 19B) shows an elevated magnetic signature for the Finlayson rock unit, as expected, in agreement with rock property measurements. The remainder of the unconstrained susceptibility inversion model shows low to very low magnetism with the lowest values centred on the Snowcap rock unit.

The geologically constrained magnetic inversion model results for cross-section A-A' (Fig. 19 C and D) show a good match between the reference and inversion results for the sediments, Finlayson, and Snowcap rock units. However, the western half of the magnetic model section shows moderate magnetic susceptibility values for the Shonektaw, Nakina, and Cache Creek rock units—rock bodies that we expected to have uniformly low magnetic signatures. Clearly the inversion model is unable to distinguish between these three rock units, but the results also suggest that there is more magnetic material in these units than implied by existing rock property measurements. An alternative explanation would be that the floor of Teslin Lake is covered by a thicker section of magnetic lake sediments; however, such a scenario would likely impose too much low-density material and be inconsistent with the gravity data.

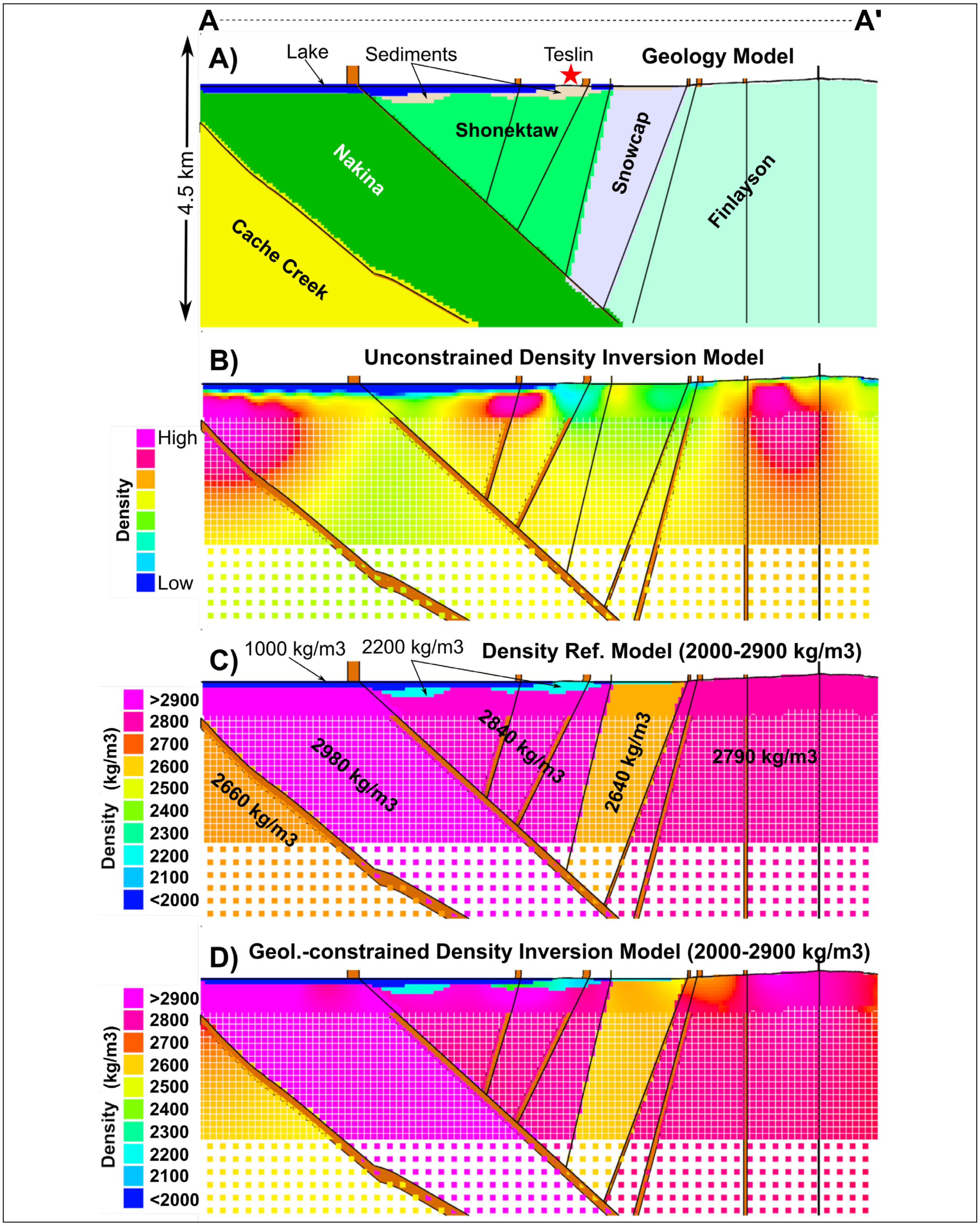

Figure 17. *Geology and density cross-sections along A-A' through the Village of Teslin using the lower density colour ramp (2000–2900 kg/m*^{3}*).* ***A)*** *Reference geology model with rock units labeled.* ***B)*** *Unconstrained density inversion model result, which is free of the influence of geology, with a qualitative colour ramp.* ***C)*** *Reference rock density model used as constraints on the modelling.* ***D)*** *Rock density distribution returned by the 3D gravity inversion modelling that honours the gravity data. The colour scale for (C) and (D) is at the lower end of the density range (2000–2900 kg/m*^{3}*) to visualize the lower density sedimentary rocks in the area. The match between the reference rock density model (C) and the inverted rock density model (D) is good. See text for further explanation.*

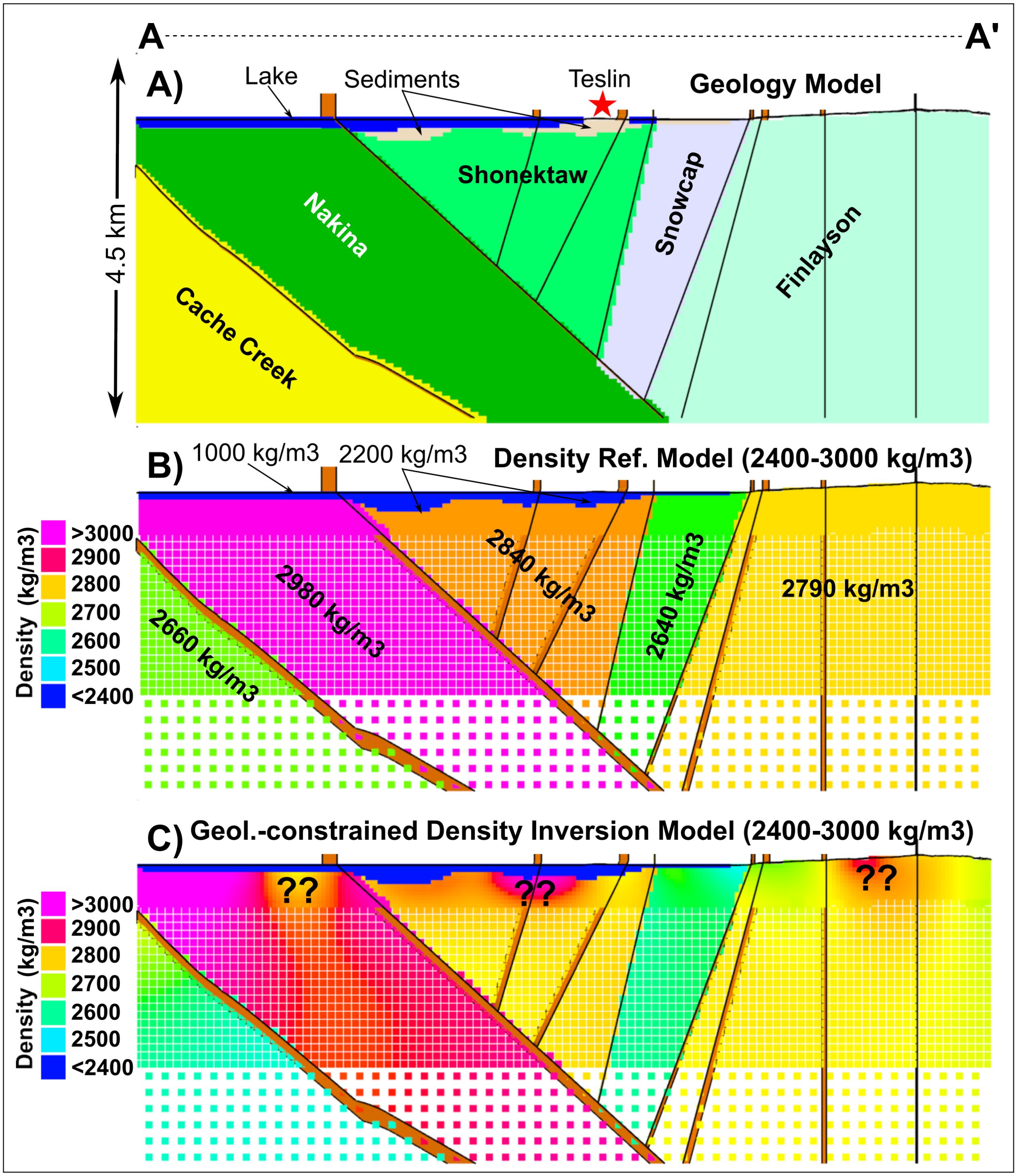

Figure 18. *Geology and density cross-sections along A-A' through the Village of Teslin using the higher density colour ramp (2400–3000 kg/m³).* ***A)*** *Reference geology model with rock units labeled.* ***B)*** *Reference rock density model used as constraints on the modelling.* ***C)*** *Rock density distribution returned by the 3D gravity inversion modelling that honours the gravity data. The colour scale for (B) and (C) is at the higher end of the density range (2400–3000 kg/m³) to visualize the higher density bedrock lithologies in the area. In this view, the match between the reference rock density model (B) and the inverted rock density model (C) is mostly good except for a few areas. Locations where mismatches occur (marked by ??) need more information to help better understand the subsurface. See text for further explanation.*

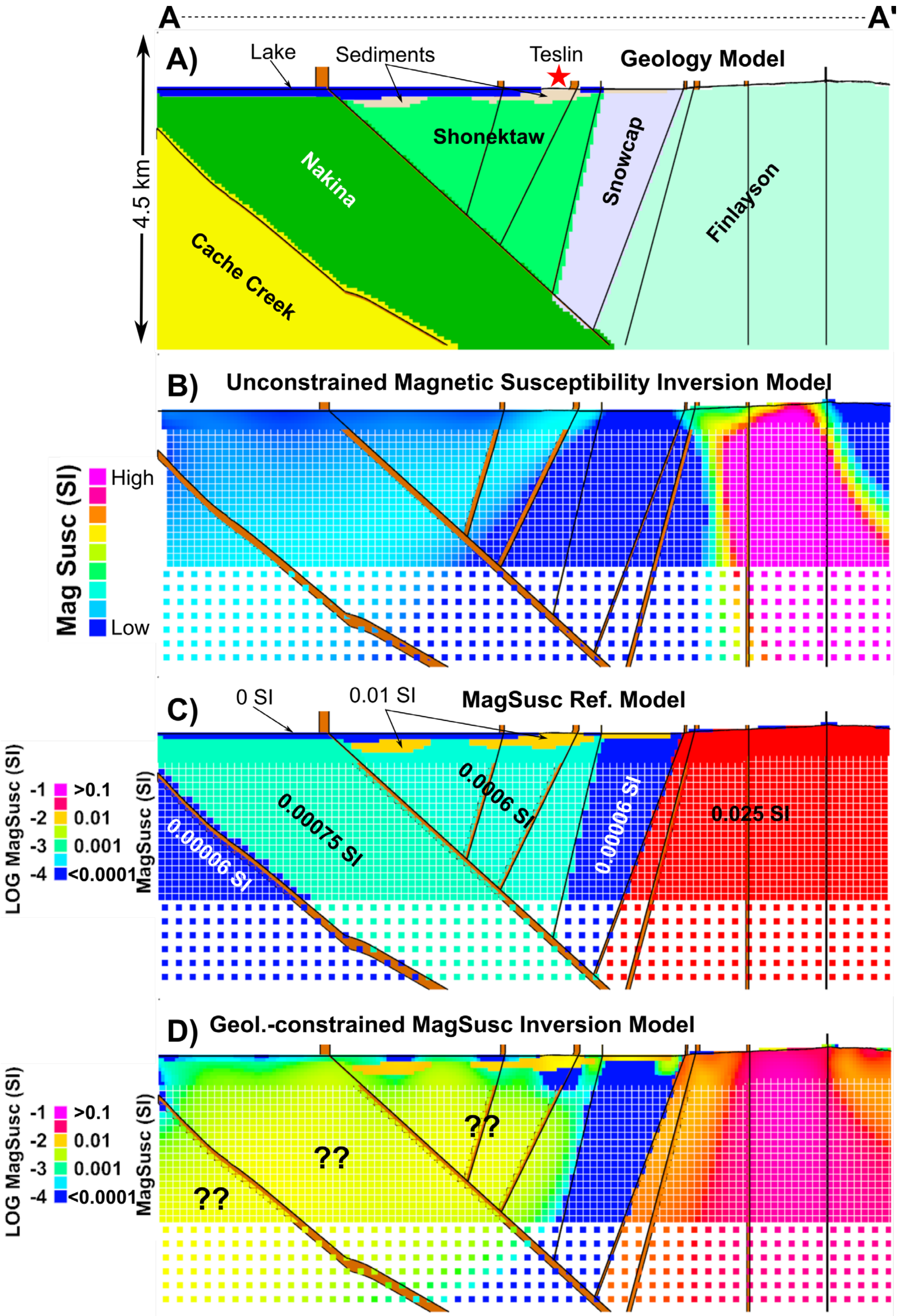

Figure 19. *Geology and magnetic susceptibility cross-sections along A-A' through the Village of Teslin.* ***A)*** *Reference geology model with rock units labeled.* ***B)*** *Unconstrained magnetic susceptibility inversion model result, which is free of the influence of geology, with a qualitative colour ramp.* ***C)*** *Reference rock magnetic susceptibility model used as constraints on the modelling.* ***D)*** *Rock magnetic susceptibility distribution returned by the 3D magnetic inversion modelling that honours the magnetic survey data. A log scale is used for the magnetic susceptibility values to help better visualize the results. The match between the reference rock susceptibility model (C) and the inverted rock susceptibility model (D) is good in some areas but not in others.*

Explanation of cross-section B-B': through the NE-SW trough at Fox Creek

Cross-section B-B' was selected to pass through the northeast-southwest sediment-filled trough inferred in the Fox Creek valley. This cross-section contains five out of the seven rock units found in the study area and a handful of faults (Fig. 20A). Key features of the geology model in this area include: 1) near-vertical contacts bounding the Snowcap assemblage; and 2) normal faults within the Shonektaw Formation that bound a zone of extension that is filled with sediments. Sediments are very thin in other parts of this cross-section.

The unconstrained density inversion model (Fig. 20B) clearly shows a broad zone of low density within the Shonektaw unit, which guided placement of the low-density sediments there. Similarly, as expected, the Shonektaw and Finlayson rock units are largely characterized by high density. The Snowcap assemblage, however, shows a rather varied distribution of density, which is puzzling.

The geologically constrained density inversion model for cross-section B-B' show an uneven match between the reference and inversion results (Fig. 20 C and D). For example, the model result suggests that the sediments in the Fox Creek valley could be even lower density (or thicker). The modelled sediment in the trough already has a maximum thickness of ~350 m; even more low-density sediment seems geologically unlikely. The density inversion model results with an alternate colour scheme (Fig. 21 B and C) show a small, dense shallow body on the west side of the Shonektaw rock unit surrounded by material which is substantially lower density than expected (*i.e.*, ~2700 kg/m^3 vs. 2840 kg/m^3). The dense body could be explained by another pocket of ultramafic rocks, but the large area of low density in the Shonektaw suggests a different sub-lithology in this unit (i.e. mostly sedimentary rock vs. mostly volcanic rock?). The density model results for the Snowcap assemblage (varying from 2500 kg/m^3–2900 kg/m^3) are even more difficult to explain. Rock property measurements on samples from the Snowcap assemblage include high density lithologies up to ~2800 kg/m^3 (*i.e.*, not quartzite; Table 1) and these could explain the high-density regions observed here. However, the unusually low-density region modelled for the Snowcap (*i.e.*, even lower density than quartzite) suggests that the geologic boundaries of the Snowcap are likely not quite right.

The unconstrained magnetic susceptibility inversion model for B-B' (Fig. 22B) shows an elevated magnetic signature for the Finlayson rock unit, consistent with rock property measurements. In addition, a zone of slightly elevated magnetic susceptibility is shown where the sediment-filled trough is located; all other areas show very low magnetism.

The geologically constrained magnetic inversion model results for section B-B' (Fig. 22 C and D) show a good match between the reference and inversion results for the Snowcap and Finlayson units. A mismatch exists in a couple areas for the Snowcap unit which suggests that the geologic boundaries may not be correctly positioned (like the conclusion made about the density model for this cross-section). The match between the magnetic reference and inversion models for the Shonektaw unit is poor, most likely because the inversion algorithm has difficulty resolving such low magnetic susceptibility variations. An alternative explanation is that the reference susceptibility of the sediments (*i.e.*, 0.01 SI) has been set too high, thus artificially creating a near-zero region of susceptibility beneath it. Rock property measurements on the near surface sediments would be a great aid in this regard.

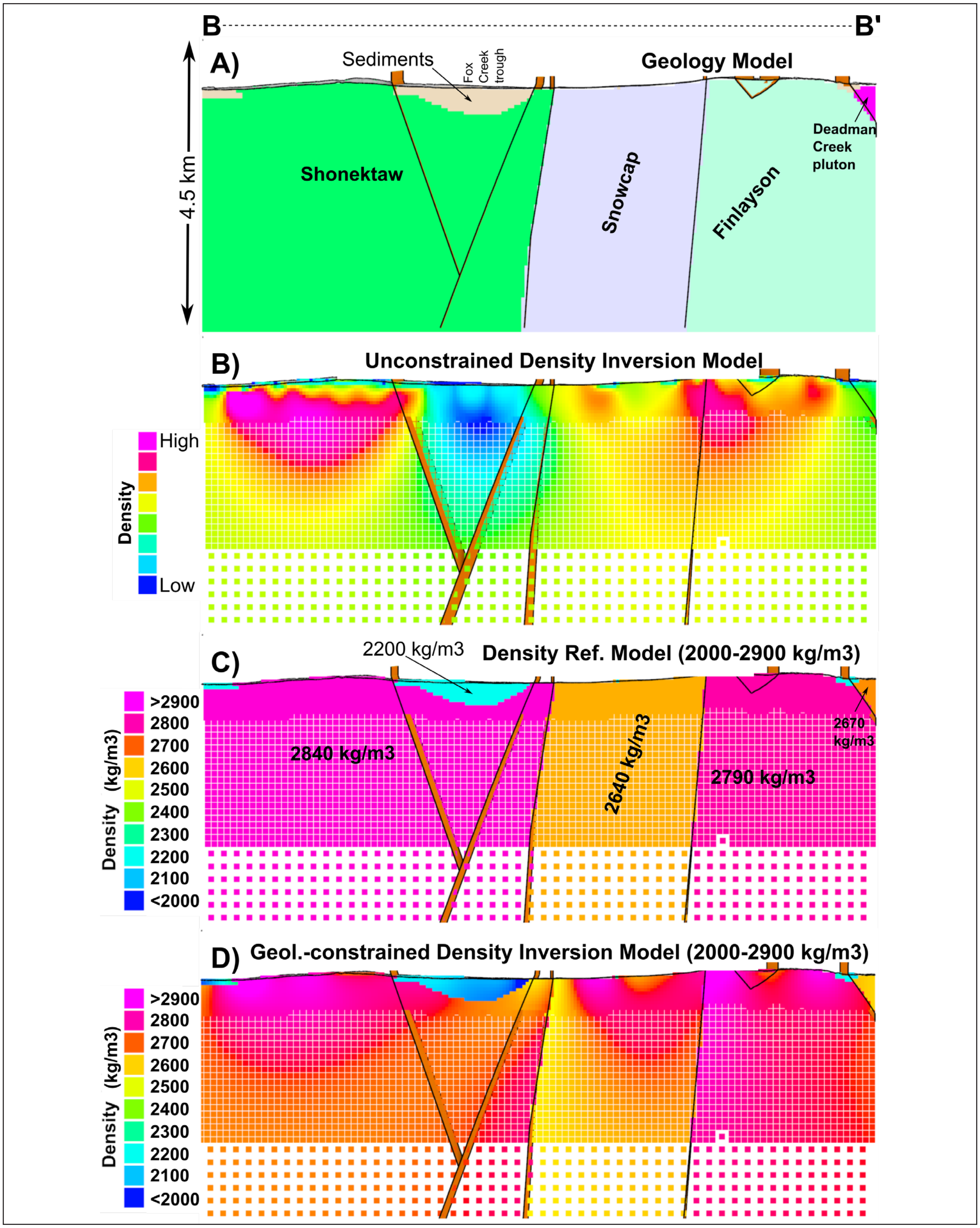

Figure 20. *Geology and density cross-sections along B-B' using the lower density colour ramp (2000–2900 kg/m*^{3}*).* ***A)*** *Reference geology model with rock units labeled.* ***B)*** *Unconstrained density inversion model result, which is free of the influence of geology, with a qualitative colour ramp.* ***C)*** *Reference rock density model used as constraints on the modelling.* ***D)*** *Rock density distribution returned by the 3D gravity inversion modelling that honours the gravity data. The colour scale for (C) and (D) is at the lower end of the density range (2000-2900 kg/m3) to visualize the lower density sedimentary rocks in the area. The match between the reference rock density model (C) and the inverted rock density model (D) appears to be good in some areas but not in others. See text for further explanation.*

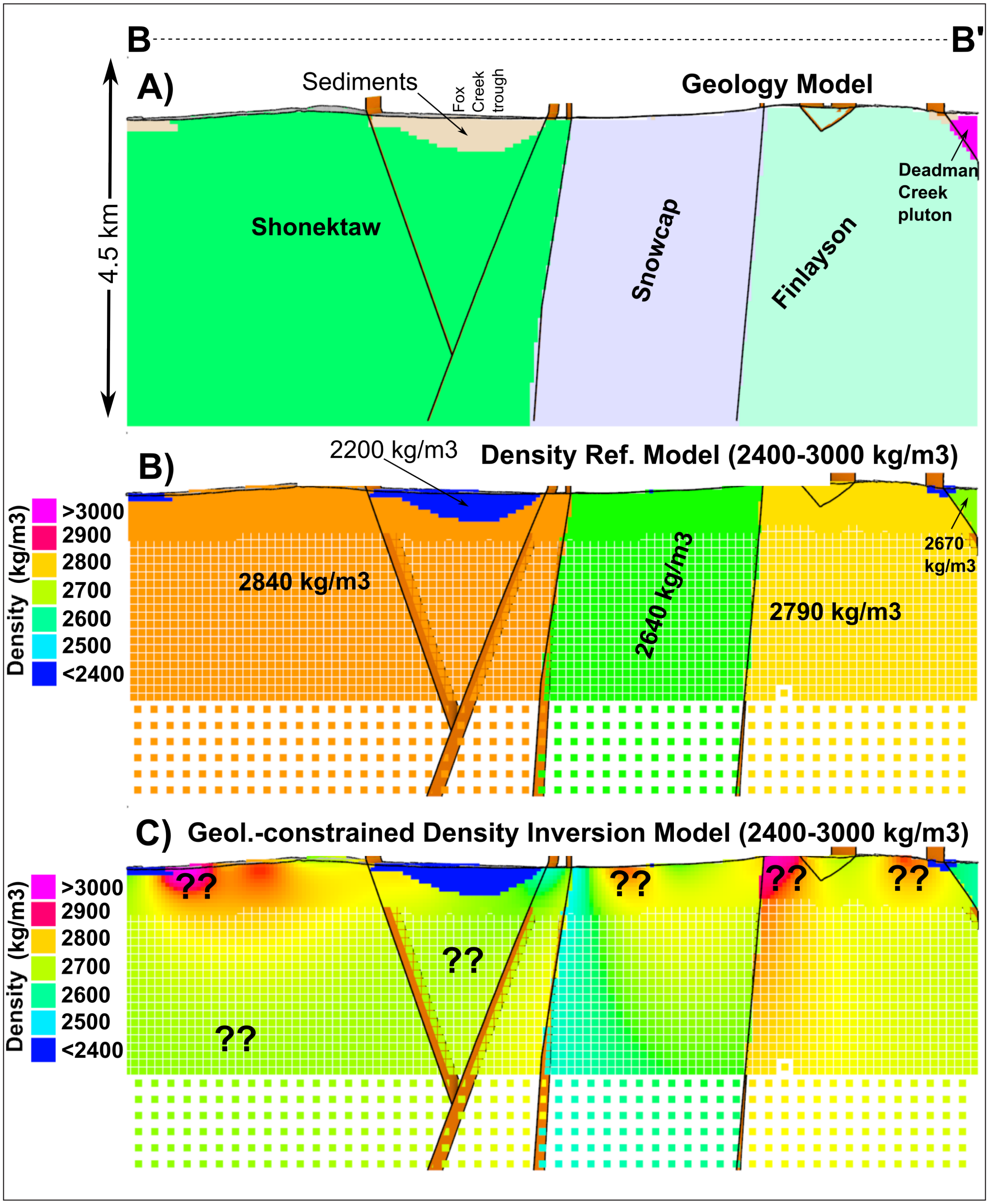

Figure 21. *Geology and density cross-sections along B-B' using the higher density colour ramp (2400-3000 kg/m3). A) Reference geology model with rock units labeled. B) Reference rock density model used as constraints on the modelling. C) Rock density distribution returned by the 3D gravity inversion modelling that honours the gravity data. The colour scale for (B) and (C) is at the higher end of the density range (2400-3000 kg/m3) to visualize the higher density bedrock lithologies in the area. The match between the reference rock density model (B) and the inverted rock density model (C) is not very good in several areas. This means that the subsurface geology is more complicated than shown here.*

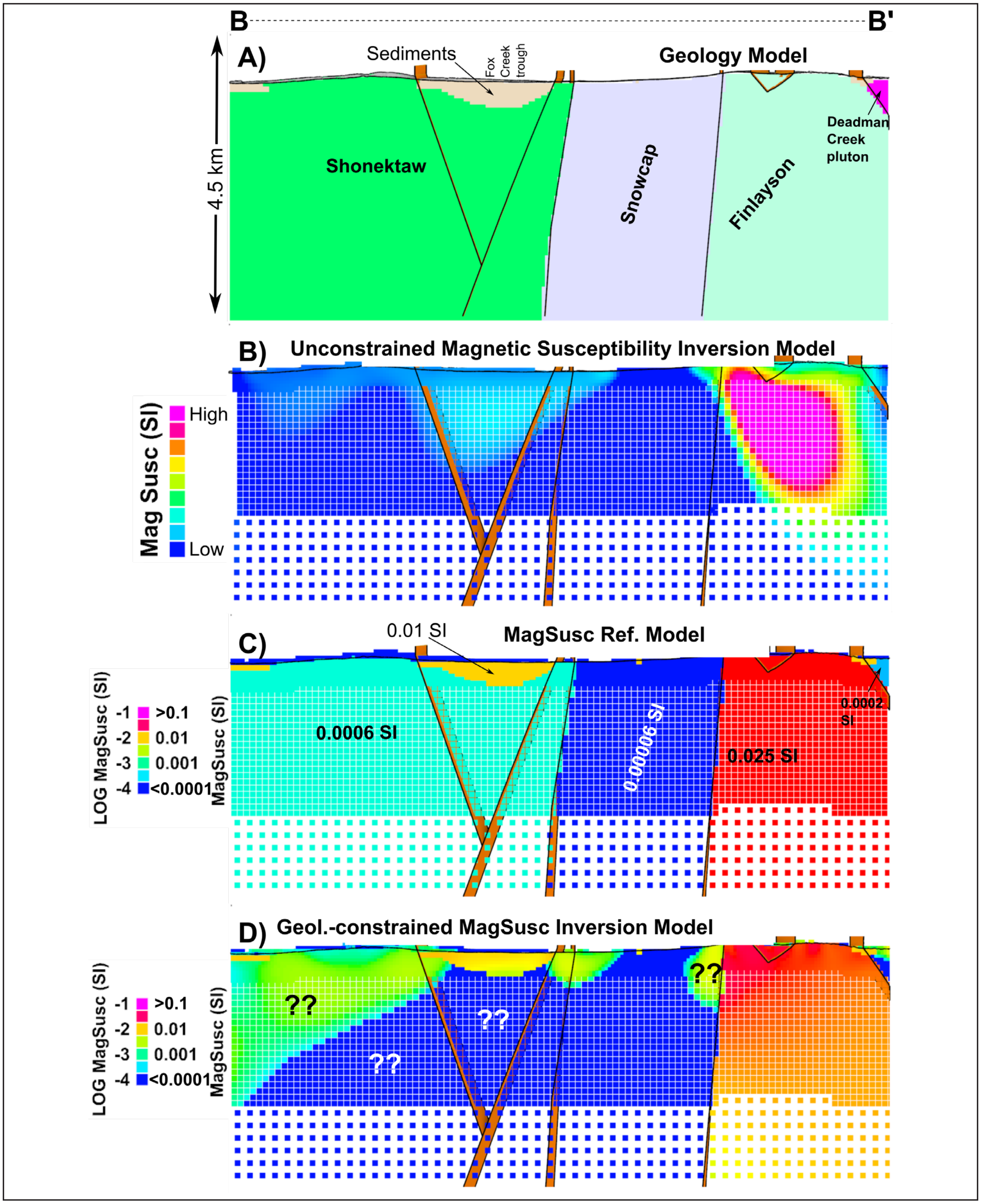

Figure 22. *Geology and magnetic susceptibility cross-sections along B-B'.* ***A)*** *Reference geology model with rock units labeled.* ***B)*** *Unconstrained magnetic susceptibility inversion model result, which is free of the influence of geology, with a qualitative colour ramp.* ***C)*** *Reference rock magnetic susceptibility model used as constraints on the modelling.* ***D)*** *Rock magnetic susceptibility distribution returned by the 3D magnetic inversion modelling that honours the magnetic survey data. A log scale is used for the magnetic susceptibility values to help better visualize the results. The match between the reference rock susceptibility model (C) and the inverted rock susceptibility model (D) is good in many areas but not in others.*

Overall, this 3D modelling exercise has revealed a fair, but incomplete, understanding of the structure and bedrock distribution in the Teslin study area. On a broad scale, the contacts between the major rock units largely agree with the gravity and magnetic modelling. Similarly, the gravity and magnetic modelling suggest that evidence is strong for a northeast-southwest oriented, sediment filled trough at Fox Creek; details such as the exact thickness and actual rock property values for the sediment layer, however, remain elusive and require additional data. Lithologic variations within rock units are also clearly present; to more fully explain them additional investigation is needed (*e.g.*, geologic mapping, rock property measurements, etc.). As is often the case, the geologic framework in the Teslin area is more complex than what we can depict here.

Discussion – implications for geothermal resources

Temperature

This project did not obtain any new measurements of subsurface temperature in the Teslin area. The only estimates suggesting favourable subsurface temperatures in the Teslin area is elevated heat flow on a regional scale for southern Yukon (Lewis *et al.*, 2003) and above average crustal-scale temperature gradient values (~45 °C/km) estimated from Curie Point depth measurements (Li *et al.*, 2017; Witter *et al.*, 2018). The drilling of an exploratory borehole is needed to find out if the subsurface in the Teslin area is actually warm.

Permeability

Rock permeability, in addition to elevated temperature, is a key requirement for a conventional (*i.e.*, not engineered) geothermal system to be viable. This study has revealed evidence for a network of faults with orientations that could favour opening of permeable structures in the subsurface along which geothermal fluids could possibly ascend to shallower levels.

Fracture Permeability

One of the key goals of this project was to try to find permeability associated with the Teslin fault zone that could potentially host upwelling geothermal fluids in bedrock. The 3D geologic model reveals evidence for geologic structures that are more complex than previously mapped. More importantly, the geologic structures identified are analogous to favourable geothermal settings found elsewhere (*e.g.*, Faulds and Hinz, 2015). Specifically, the structural setting found in the Teslin area has similarities to a strike-slip duplex (Woodcock and Fischer, 1986) within a bifurcating strike-slip fault zone (Fig. 4). The global analogue for this structural environment is the “equatorial bifurcation zone” along the Sumatran fault in Indonesia (Sieh and Natawidjaja, 2000; Weller *et al.*, 2012). The Sumatran fault is a major, right-lateral, crustal scale fault associated with oblique, north-dipping subduction. This fault has a major irregularity near the equator where the fault splits into two sub-parallel strands up to 35 km apart. Studies of the seismicity along this section of the Sumatran fault describe a complex network of strike-slip shears and conjugate Riedel shears that together form the bifurcation zone (Fig. 4; Weller *et al.*, 2012). A similar structural framework may be present in the Teslin area.

A key feature of a strike-slip duplex within a bifurcating strike-slip fault zone is that some of the faults can accommodate extensional motion and form small pull-apart basins where fractured rock and permeability are likely to form. The geophysical evidence and interpretation presented here suggests that the northeast-southwest sediment-filled trough at Fox Creek is a key structural component of the proposed strike-slip duplex structural framework.

Specifically, the northeast-southwest trough may have formed due to extensional tectonics associated with motion along and within the bifurcated Teslin fault zone. We propose that a small pull-apart was formed in the vicinity of the present-day Fox Creek creating permeable, fractured rocks in the subsurface. Therefore, it is in the vicinity of the Fox Creek valley that the conditions would be more favourable to look for subsurface permeability.

The highly complex structural environment inferred for the Teslin fault zone likely hosted extensive subsurface permeability in the distant past during periods of active tectonism (e.g., the Cretaceous Period). Unfortunately, the Teslin fault zone appears to be inactive today. Furthermore, in many cases, subsurface fracture permeability generated by faulting and tectonism gets resealed during post-emplacement hydrothermal fluid circulation and mineral precipitation. If that has occurred in the Teslin fault zone, then subsurface permeability in the area may be poor. However, the fault network identified in the Teslin area could still host subsurface permeability today, despite a lack of robust tectonism, like that observed in the geothermal areas of the southern Canadian Rockies (*e.g.*, Grasby and Hutcheon, 2001). In summary, fracture permeability at Teslin is possible and it should be tested with exploratory drilling.

Stratigraphic Permeability

An alternative to fracture permeability in geothermal systems is stratigraphic permeability. Stratigraphic permeability involves horizontal layers of porous and permeable rock, lying at significant depth below the surface (*i.e.*, > 1 km), in which warm geothermal fluids could reside. Good examples of such rock types would be clean, quartz-rich sandstones and karstic carbonate rocks (*e.g.*, limestone with portions of it dissolved away). Evidence from this study suggests that sediment cover in the Teslin area is quite thin (e.g., a few tens of metres or less) almost everywhere. The exception is the northeast-southwest trough where sediment thickness may be up to a few hundred metres thick. Evidence for structurally controlled and relatively deep (*i.e.*, > 1 km) sedimentary basins is lacking in the Teslin area.

Thick sections of sedimentary rocks are found in the Cache Creek terrane (located in the southwest corner of the study area) including carbonate and sandstone lithologies. This raises the question whether stratigraphic permeability could exist there. This study did not identify evidence for or against permeability in the Cache Creek terrane. However, the location of these rock units on the far side of Teslin Lake in a relatively inaccessible area makes a potential geothermal resource of limited interest.

Permeability at Intrusive Contacts

Another possible area of subsurface permeability in the Teslin area could be at the geologic contact between igneous intrusions and country rock. This can happen because igneous intrusions are emplaced at elevated temperatures, and upon cooling, thermal contraction can create permeability along the margins of the igneous intrusion (Gilbert *et al.*, 2018).

Unfortunately, the only igneous intrusion near Teslin is the Deadman Creek pluton (located in the northeast corner of the study area) which is relatively far from any access roads. Geophysical modelling in this study largely supports the current mapped location of the pluton contact. But due to the remote location, drilling into the margin of the Deadman Creek pluton to test for subsurface permeability would involve challenging access and high expense. Furthermore, if warm geothermal fluids were found near the Deadman Creek pluton, they are several kilometres from the Village of Teslin, which would add to development costs. Lastly, radiogenic heat production measurements on rock samples from the Deadman Creek pluton show that this rock unit has low potential for generating additional heat.

Proposed Drilling Target

The new geoscience data and modelling performed for this study have identified a prospective location for a scientific research well that could provide information about subsurface temperature and permeability (Figs. 23 and 24). The proposed well location lies at the intersection of two faults inferred from this study: a northwest-trending strike-slip fault and a northeast-trending normal fault. The northeast-trending normal fault forms the southern boundary of the Fox Creek trough. Fault intersections can be favourable drilling locations because they are more likely to have fractured, permeable rocks that can allow ascent of warm geothermal fluids. In addition, the subsurface bedrock geology at the proposed location is expected to be volcanic rocks of the Shonektaw Formation (based upon nearby rock outcrops). Unlike shale and other clay-rich rocks, faulted volcanic rocks have the potential to maintain open fractures that would promote permeability. Lastly, to facilitate access for a drilling rig, the proposed site is located next to an existing road.

The proposed drill site is located ~500 m north of the Alaska Highway and ~350 m west of the sewage lagoon near the intersection of two gravel roads (latitude 60.180627° N, longitude 132.770770° W, 709 m elevation; WGS84 datum). The proposed drill site has the potential to answer the greatest number of questions about the subsurface at a single location. Key questions include:

- Is there a fault in the subsurface at this location?
- How thick is the sedimentary cover at the proposed drill site?
- What type of bedrock underlies the sedimentary materials at the drillsite and are they fractured/permeable?
- What is the temperature gradient and heat flow at the drillsite?
- If water is encountered in the well, what does the subsurface water chemistry tell us about the temperature of potential geothermal source aquifers? (*i.e.*, geothermometry)

The proposed depth of the research well is 500 m. Some advantages of this proposed drill site include:

- there is unimpeded road access to the proposed drill location;
- although the drill site has not been visited by the author, according to satellite images, the proposed drill site has few trees and appears to have a gentle slope;
- the location lies above a normal fault inferred from the gravity and magnetic data;
- a drilling depth of 500 m would most likely penetrate through the sedimentary cover and into the underlying bedrock. According to the 3D geologic model presented in this study, a borehole at the proposed location would drill through ~150 m of near surface sediments and ~350 m of Shonektaw Formation bedrock (primarily volcanic rocks); and
- a depth of 500 m would be sufficient to measure the subsurface temperature gradient with a high degree of accuracy, avoiding any near-surface or paleoclimate/permafrost effects.

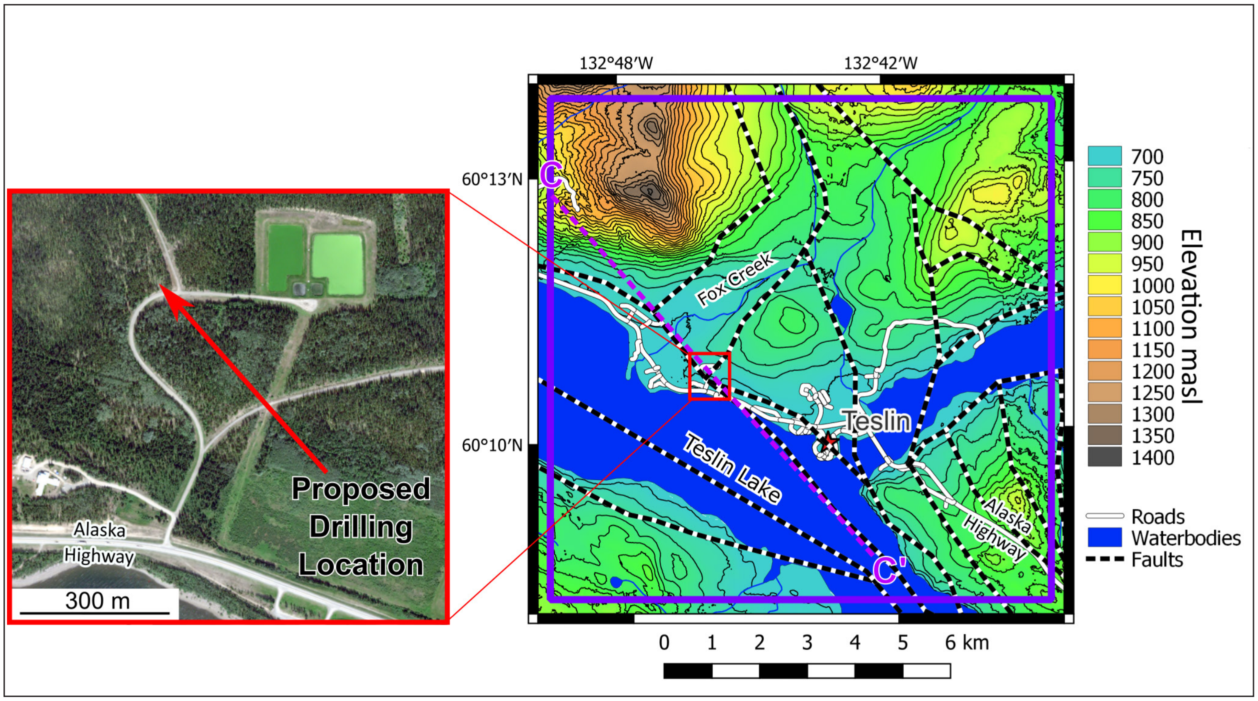

Figure 23. *Map showing the proposed location of the scientific research well for the Teslin study area. The proposed location lies at the intersection of a northwest-trending splay of the Teslin fault and a northeast-trending normal fault bounding the sediment-filled trough at Fox Creek. The map on the right shows the location of cross-section C-C' (purple dash line; see Figure 24). The inset (red box on the left) shows a satellite image with the proposed drilling location identified.*

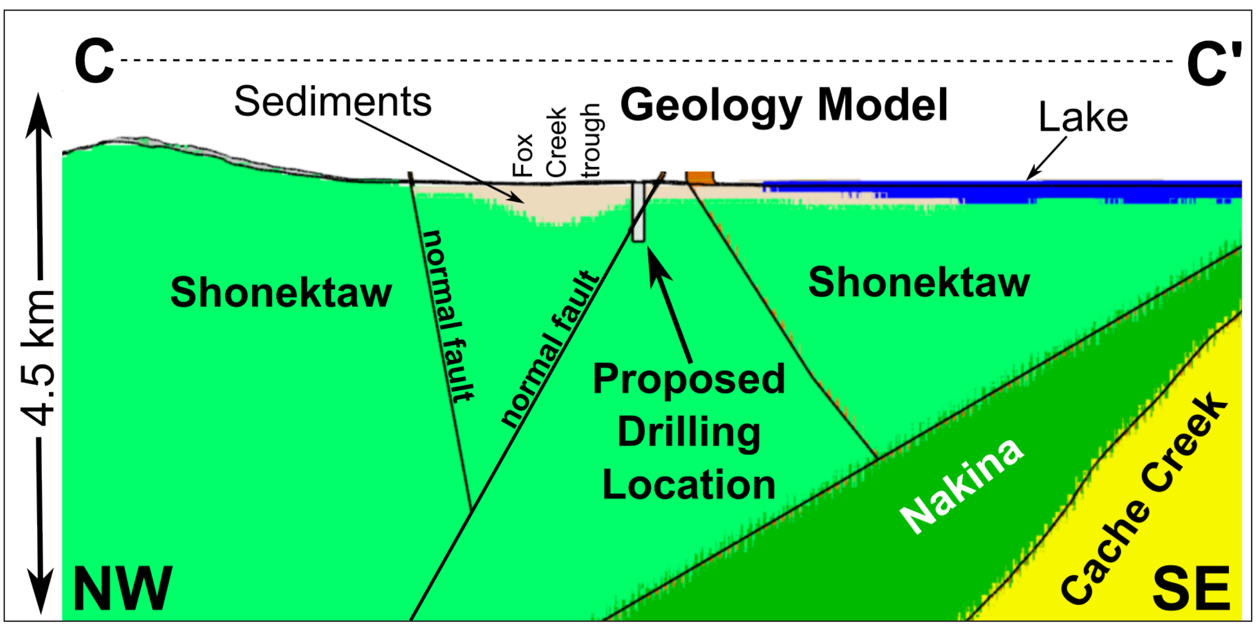

Figure 24. *Cross-section C-C' showing the proposed location of a 500m deep scientific research well (thick grey line) for the Teslin study area. According to the 3D geology model, a borehole at the proposed location would drill through ~150 m of near surface sediments and ~350 m of Shonektaw Formation bedrock (primarily volcanic rocks). A zone of faulted rock would be encountered at a depth of ~300 m. The cross-section is ~10 km long, oriented northwest-southeast, and the location is shown in Figure 23.*

Conclusions

This study analyzed and interpreted an array of geoscience data near the Teslin fault zone and the Village of Teslin in southern Yukon. The primary aim of the study was to better understand the potential for geothermal energy resources in the area in the context of subsurface temperature and permeability. Interest in the geothermal potential near Teslin has arisen due to: 1) a need to reduce the dependence on fossil fuels used for heat and power by the residents of Teslin; 2) the presence of the large Teslin fault zone (which suggests the possibility of fractured rock and permeability in the subsurface); and 3) evidence for above average temperature gradients and elevated heat flow at the regional scale. Key geoscience datasets interpreted in this study include: bedrock geology maps, surficial geology maps, fault maps, rock properties, gravity data, magnetic survey data, audio-magnetotelluric data, LiDAR topographic data, as well as water well data.

A map-based investigation of these data revealed a complex network of faults that appear to form a strike-slip duplex between the two bifurcating strands of the Teslin fault zone. Coincident gravity and magnetic anomalies, oriented northeast-southwest, at Fox Creek are interpreted as a small, sediment-filled, pull-apart trough bounded by northeast-trending normal faults. Geologically constrained 3D modelling of the gravity and magnetic data provide supporting evidence for this interpretation. Extensional tectonics, as inferred for this pull-apart trough, are important for geothermal systems because they can generate subsurface regions of permeable, fractured rock.

This study proposes a drilling location to test subsurface temperature and permeability. The proposed drill site is located at an inferred fault intersection on the edge of the northeast-southwest pull-apart trough near Fox Creek. The proposed drill site also has road access. The drilling of a research well at the proposed site could help answer two key questions about the subsurface in the Teslin area that remain unanswered:

- What is the actual temperature gradient in the Teslin area?
- Is the bedrock in the complex network of faults in the Teslin fault zone fractured and permeable?

The recommended drilling depth of the proposed scientific research well is 500 m. The key data sets to be obtained from this research well include: downhole geology, water samples, and an equilibrated static temperature profile.

Recommendations

This geothermal study has been able to leverage large amounts of pre-existing, high quality geoscientific data. Additional data collection and analysis would be helpful to better understand the subsurface in the Teslin area. The drilling of a scientific research well proposed in this report would answer many questions about the subsurface in the region. Additional geoscientific studies that could be helpful include:

- collection of airborne ZTEM (Z-axis Tipper Electromagnetic) data followed by 3D resistivity modelling of the ZTEM data would provide full data coverage of the Teslin study area (especially in difficult to access areas far from roads). One possible outcome of a 3D resistivity model study with ZTEM data is that it could help better define the distribution and thickness variations of the near surface sediment layer. One focus of such an effort could be to try and differentiate the blanket of glacial sediments from other sediment packages that get deposited as a result of small-scale extensional tectonics within the Teslin fault zone; and
- additional geologic mapping and rock property data collection in the Teslin study area would help to better refine our understanding of bedrock distribution and lithologic variation within the major rock units.

Acknowledgements

This project benefited greatly from discussions with: Maurice Colpron about bedrock geology and structure of southern Yukon, Panya Lipovsky about surficial geology in the Teslin area, as well as Jim Craven and Victoria Tschirhart about the Teslin AMT survey and resistivity model. Special thanks to Maurice Colpron for a helpful review of this report which improved the text.

References

Cockett, R., Kang, S., Heagy, L.J., Pidlisecky, A., Oldenburg, D.W., 2015. SimPEG: An open-source framework for simulation and gradient based parameter estimation in geophysical applications. Computers and Geosciences, vol. 85, p. 142–154.

Colpron, M., 2019. Potential radiogenic heat production from granitoid plutons in Yukon. Yukon Geological Survey, Open File 2019-16, 1 map and data.

Colpron, M., 2022. Yukon Bedrock Geology Map. Yukon Geological Survey, Open File 2022-1, scale 1:1 000 000, 2 sheets.

Colpron, M., Hayward, N., Crowley, J.L., 2021. Potential heat production from the Seagull and Teslin plutonic suites, southern Yukon: Geochemistry, geochronology, rock physical properties, and 3D geophysical inversion of Bouguer gravity data. In: Yukon Exploration and Geology 2020, K.E. MacFarlane (ed.), Yukon Geological Survey, p. 47–72.

Dehkordi, B.H., Ferguson, I.J., Jones, A.G., Ledo, J., Wennberg, G., 2019. Tectonics of the northern Canadian Cordillera imaged using modern magnetotelluric analysis. Tectonophysics, v. 765, p. 102-128.

Faulds, J.F., Hinz, N.H., 2015. Favorable Tectonic and Structural Settings of Geothermal Systems in the Great Basin Region, Western USA: Proxies for Discovering Blind Geothermal Systems. Proceedings World Geothermal Congress, Melbourne, Australia, 19–25 April 2015, 6 pages.

Fournier, D., Oldenburg, D., 2019. Inversion using spatially variable mixed Lp norms. Geophysical Journal International, vol. 218, p. 268–282.

Fullagar, P.K., Pears, G.A., 2007. Towards geologically realistic inversion. Proceedings of Exploration 07: Fifth Decennial International Conference on Mineral Exploration, Toronto. p. 444–460.

Fullagar, P.K., Pears, G.A., McMonnies, B., 2008. Constrained inversion of geologic surfaces—Pushing the boundaries. The Leading Edge, vol. 27, p. 98–105.

Gabrielse, H., Murphy, D.C., Mortensen, J.K., 2006. Cretaceous and Cenozoic dextral orogeny parallel displacements, magmatism and paleogeography, north-central Canadian Cordillera. In: Haggart JW, Monger JWH, Enkin RJ, (eds.), Paleogeography of the North American Cordillera: Evidence For and Against Large-Scale Displacements: Geological Association of Canada, Special Paper 46, p. 255-276.

Gilbert, L.A., Crispini, L., Tartarotti, P., Bona, M.L., 2018. Permeability Structure of the Lava-Dike Transition of 15 Myr Old Oceanic Crust Formed at the East Pacific Rise. Geochemistry, Geophysics, Geosystems, v. 19, p. 3555-3569.

Gordey, S.P., 1991. Teslin map area, a new geological mapping project in southern Yukon. In: Current Research, Part A, Geological Survey of Canada, Paper 91-1A, p. 171-178.

Gordey, S.P., Stevens, R.A., 1994. Preliminary interpretation of bedrock geology of the Teslin area (105C), southern Yukon: Geological Survey of Canada Open File 2886, (map, scale 1:250 000).

Government of Yukon, 2018. Yukon's Energy Context. Energy Branch, Department of Energy, Mines, and Resources, 12 pages, https://yukon.ca/sites/yukon.ca/files/emr/emr-yukon-energy-context.pdf.

Grasby, S.E., Hutcheon, I., 2001. Controls on the distribution of thermal springs in the southern Canadian Cordillera. Canadian Journal of Earth Sciences, v. 38, p. 427-440.

Hasterok, D., Webb, J., 2017. On the radiogenic heat production of igneous rocks. Geoscience Frontiers, vol. 8, p. 919-940.

Hyndman, R.D., Cassidy, J.F., Adams, J., Rogers, G.C., Mazzotti, S., 2005. Earthquakes and Seismic Hazard in the Yukon-Beaufort-Mackenzie. Recorder, v. 30, no. 5, 16 pages.

Kiss, F., Boulanger, O., 2018. Residual Total Magnetic Field, Aeromagnetic Survey of the Marsh Lake Area, Yukon, Part of NTS 105-C/South; Geological Survey of Canada, Open File 8412; Yukon Geological Survey Open File 2018-3, Scale 1:100 000.

Larson, K., 2002. Microstructural Analysis of the Teslin fault, Northwestern British Columbia. British Columbia Geological Survey, Geological Fieldwork 2001, Paper 2002-1, 4 pages.

Leonard, L.J., Mazzotti, S., Hyndman, R.D., 2008. Deformation rates estimated from earthquakes in the northern Cordillera of Canada and eastern Alaska. Journal of Geophysical Research, vol. 113, B08406, doi:10.1029/2007JB005456.

Lewis, T.J., Hyndman, R.D., Flück, P., 2003. Heat flow, heat generation, and crustal temperatures in the northern Canadian Cordillera: Thermal control of tectonics. Journal of Geophysical Research, v. 108, no. B6, 2316, doi:10.1029/2002JB002090.

Li, C.-F., Lu, Y., Wang, J., 2017. A global reference model of Curie-point depths based on EMAG2. Nature, Scientific Reports, v. 7 DOI: 10.1038/srep45129, 9 pages.

Mihalynuk, M.G., Friedman, R.M., Devine, F. and Heaman, L.M., 2006. Protolith age and deformation history of the Big Salmon complex, relicts of a Paleozoic continental arc in northern British Columbia. In: Paleozoic Evolution and Metallogeny of Pericratonic Terranes at the Ancient Pacific Margin of North America, Canadian and Alaskan Cordillera, M. Colpron and J.L. Nelson (eds.), Geological Association of Canada, Special Paper 45, p. 179-200. Morison, S.R., Klassen, R.W., 1997. Surficial geology, Teslin, Yukon Territory, Geological Survey of Canada, Map 1891A, scale 1:125 000.

Morison, S.R., Klassen, R.W., 1997. Surficial geology, Teslin, Yukon Territory, Geological Survey of Canada, Map 1891A, scale 1:125 000.

Sieh, K., Natawidjaja, D., 2000. Neotectonics of the Sumatran fault, Indonesia. Journal of Geophysical Research, v. 105, no. B12, p. 28,295-28,326.

Snyder, D.B., Roberts, B.J., Gordey, S.P., 2005. Contrasting seismic characteristics of three major faults in northwestern Canada. Canadian Journal of Earth Sciences, v. 42, p. 1223-1237.

Sutrisno, L., Bonet, D., Daud, Y., Smit, J., Beekman, F., Van Wees, J.D., Purwanto, W., 2019. Assessing the role of pull-apart basins for high-temperature geothermal resources in transcurrent tectonic setting: Sumatra and California compared. European Geothermal Congress 2019, Den Haag, The Netherlands, 11-14 June 2019, 9 pages.

Weller, O., Lange, D., Tilmann, F., Natawidjaja, D., Rietbrock, A., Collings, R., Gregory, L., 2012. The structure of the Sumatran fault revealed by local seismicity. Geophysical Research Letters, v. 39, 7 pages, doi:10.1029/2011GL050440.

White, D., Colpron, M., Buffett, G., 2012. Seismic and geological constraints on the structure and hydrocarbon potential of the northern Whitehorse trough, Yukon, Canada. Bulletin of Canadian Petroleum Geology, v. 60, no. 4, December 2012, p. 239-255.

Witter, J.B., Miller, C.A., Friend, M., Colpron, M., 2018. Curie Point Depths and Heat Production in Yukon, Canada. Proceedings 43rd Workshop on Geothermal Reservoir Engineering Stanford University, California, February 12-14, 2018, 11 pages.

Woodcock, N.H., Fischer, M., 1986. Strike-slip duplexes. Journal of Structural Geology, v. 8, no. 7, p. 725–735.

Yukon Geological Survey, 2020. Surficial Geology data set. Yukon Geological Survey, http://data.geology.gov.yk.ca/Compilation/33, Accessed February 15, 2021.

Yukon Geological Survey, 2023a. A digital atlas of terranes for the northern Cordillera. Yukon Geological Survey, http://data.geology.gov.yk.ca/Compilation/2, Accessed: June 2, 2023.

Yukon Geological Survey, 2023b. Yukon Digital Bedrock Geology. Yukon Geological Survey, http://datatest.geology.gov.yk.ca/Compilation/3, Accessed: June 2, 2023.

Zagorevski, A., van Staal, C.R., Bédard, J.H., Bogatu, A., Canil, D., Coleman, M., Golding, M.L., Joyce, N.L., Lawley, C., McGoldrick, S., Mihalynuk, M.G., Milidragovic, D., Parsons, A.J. and Schiarizza, P., 2021. Overview of Cordilleran oceanic terranes and their significance for the tectonic evolution of the northern Cordillera. In: Northern Cordillera geology: a synthesis of research from the Geo-mapping for Energy and Minerals program, British Columbia and Yukon, J.J. Ryan and A. Zagorevski (eds.), Geological Survey of Canada, Bulletin 610, p. 21-65.

Appendix 1: Detailed 3D gravity and geology model for the Village of Teslin

Introduction

A secondary goal of this project is to learn more about groundwater resources in the Village of Teslin. The primary groundwater resources utilized by the village are aquifers hosted in the near surface sedimentary layer above the top of bedrock. Currently, groundwater is supplied to the village via many shallow water wells drilled into the near surface sedimentary layer (and only one of these wells has drilled all the way to bedrock). In addition, bedrock is exposed at the surface (*i.e.*, sediment thickness = 0 m) in only one location in the village (Fig. A1-1). Thus, the variation in the thickness of the near surface sediment layer (*i.e.*, the depth-to-bedrock) is poorly known in the Village of Teslin. A depth-to-bedrock map would be helpful to identify regions likely to have greater thickness of near surface sediments to help target potential groundwater aquifers.

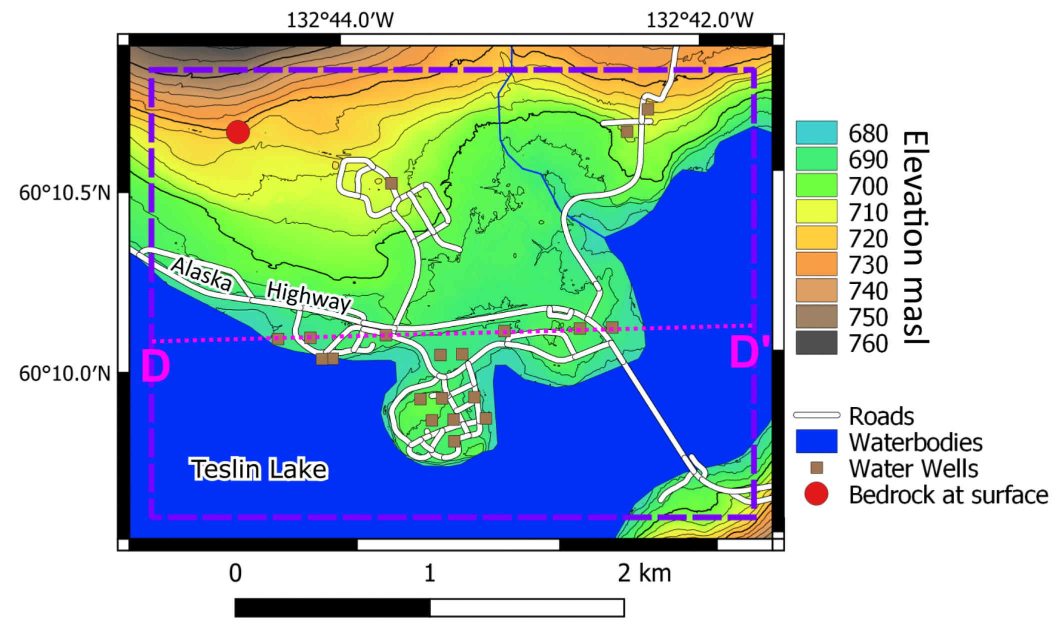

Figure A1-1. *Topography in the detailed study area (purple dashed line) where a depth-to-bedrock map was constructed. The topography shown is based upon LiDAR data with 10m contours. Locations of water wells are also plotted (brown squares) as well as one location where bedrock outcrops at the surface (red dot). Cross-section D-D' is shown in Figures A1-3 and A1-4.*

Data used for depth-to-bedrock map

As part of the 2022 Teslin gravity survey, 245 closely spaced gravity measurements were acquired in the Village of Teslin covering an area of about 1.9 km x 1.5 km in size (Fig. A1-2 and Appendix 3). These gravity measurements were spaced 100 m apart (compared to 500 m spacing in the rest of the gravity survey). The purpose of the tight gravity station spacing was to support a more detailed analysis of the depth-to-bedrock under the Village of Teslin.

In addition to the tightly spaced gravity data, the following additional data were used for the depth-to-bedrock analysis: LiDAR topographic data (~1 m resolution), water well data (Yukon water well registry), bedrock mapping data, rock density data, lake water bathymetry data (collected by Aurora Geosciences as part of this study; see Appendix 3), and the 3D geologic model of the larger study area (10 km x 10 km; Fig. 16) described in this report.

Methodology: 3D gravity + geology modelling

To generate the depth-to-bedrock map for the Teslin area, we used the same 3D gravity inversion modelling methods described earlier in this report in which the gravity modelling is guided by both a 3D geologic model as well as average rock density values for each geologic unit. The 3D gravity model volume is focused on the Village of Teslin and has the dimensions: 3.1 km east-west x 2.3 km north-south x 1.1 km thick. The footprint of this model volume encompasses all the 100 m spaced gravity measurements plus a buffer of ~500 m around it. The 3D model mesh was made as small as practicable to maximize the detail of the depth-to-bedrock map. The model mesh consists of cubic cells of the following sizes: 10 m cells from 0–100 m depth, 20 m cells from 100–700 m depth, and 40 m cells from 700–1100 m depth. Two kilometres of padding cells were added to the model volume on the sides and bottom to minimize edge effects. A total of 268 gravity data points were used in the inversion modelling. The gravity data consisted of Complete Bouguer Anomaly gravity values with a terrain correction density of 2.67 g/cm^3. The gravity data were upward continued by 100 m prior to inversion modelling to minimize near surface effects and model artifacts.

Limitations and uncertainty in the 3D gravity modelling

Non-uniqueness is a problem in 3D geophysical modelling such that even if a geophysical model is mathematically correct and matches the surface geophysical measurements quite well, it may not necessarily be geologically correct. We try to reduce this uncertainty in the depth-to-bedrock model by simultaneously matching the gravity measurements, rock density data, and the 3D geology model. One of the key sources of uncertainty, however, is rooted in the assumptions that the rock density measurements we have: 1) are representative of the rock unit as a whole; and 2) the density of a rock unit is generally uniform without much variation laterally or vertically. These assumptions affect the outcome of the depth-to-bedrock model in the following way. In areas where the bedrock is a little denser than our assumption, our predicted depth-to-bedrock will be shallower than reality. In contrast, if the bedrock is less dense than the assumed value, the predicted depth-to-bedrock will be deeper than reality. This results in an ~10–25% estimated uncertainty in the depth-to-bedrock calculations.

Results: depth-to-bedrock modelling

For the depth-to-bedrock modelling, different rock units in the 3D geologic model were assigned reference density values based upon rock density measurements (Table 1). To improve the modelling of the near surface sedimentary layer, we selected a reference density value for the sediments that increases with depth from 2000 kg/m^3 (at the land surface) to 2200 kg/m^3 (at the bottom of the sediment pile) to reflect natural compaction due to the weight of overlying sedimentary material. In the inversion calculations, the inversion algorithm adjusted the rock density values in the model cells until a match was achieved with the measured gravity data. For the gravity modelling, a match was achieved when the root-mean-squared (RMS) misfit, calculated for the 3D density model, reached the average measurement error of the gravity survey data (*i.e.*, 0.061 mGal). The actual calculated RMS misfit obtained for the final 3D density model is 0.048 mGal. Thus, the depth-to-bedrock model output is consistent with the geophysical survey data.

The final 3D geologic model constructed for the depth-to-bedrock map contains only three different rock units: near surface sediments, Shonektaw Formation, and Snowcap assemblage. A 2D cross-section showing a slice of the density model result (Figs. A1-3 and A1-4) contains the following elements: a reference geologic model (showing rock types), a reference density

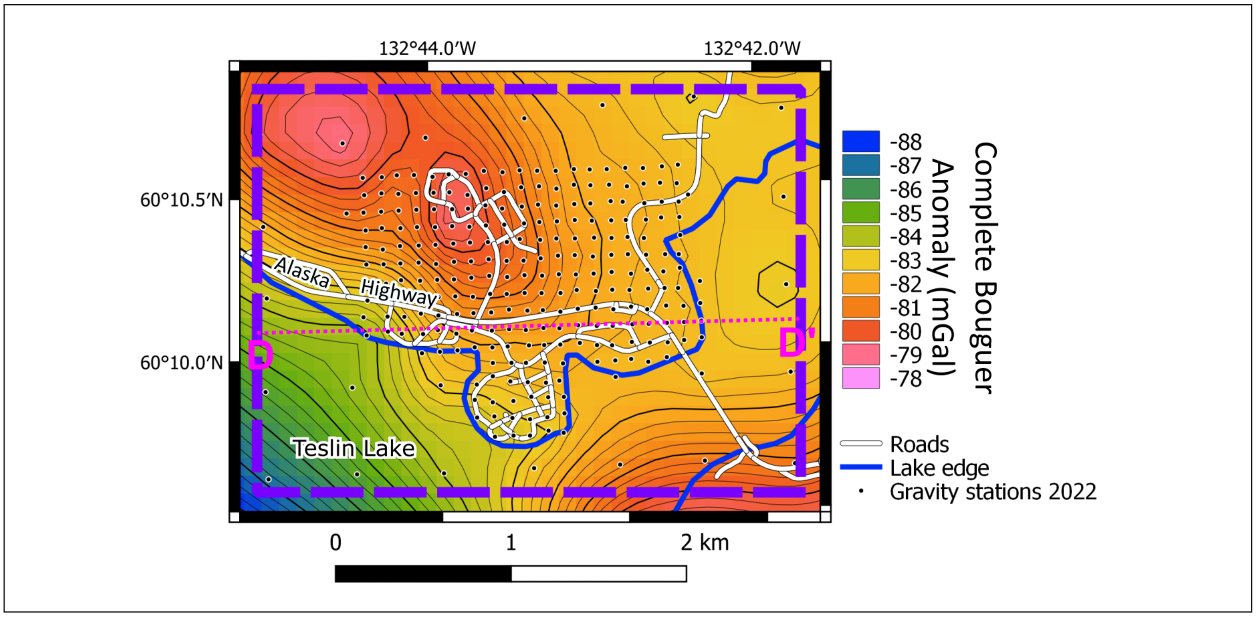

Figure A1-2. *Map showing gravity stations (black dots) within the detailed study area acquired as part of the 2022 gravity survey (Appendix 3). The study area is 3.1 km x 2.3 km (purple dashed line). However, the area covered by tightly spaced (100 m) gravity measurements is only about 1.9 km x 1.5 km in size. The background image shows the Complete Bouguer Anomaly gravity data gridded with a 100 m cell size. Gravity contours (black solid lines) are shown at 0.25 mGal intervals. The shore of Teslin Lake is shown by the thick blue line. Cross-section D-D' is shown in Figures A1-3 and A1-4.*

model (showing the values and geometry of the geologic constraints), and the geologically constrained density inversion model output (our best attempt to reconcile geology, gravity data, and rock property measurements). The density model results are presented using two colour scales (2000–2900 kg/m^3 and 2400–3000 kg/m^3) to help better visualize the lower density and higher density rock distribution in the density models.

Explanation of cross-section D-D'

Cross-section D-D' is oriented east-west and was selected to pass near the middle of the Village of Teslin and through a handful of existing water wells (Figs. A1-3 and A1-4). The model is consistent with three of the five water wells that were drilled into the sedimentary layer but did not hit bedrock (marked "1", "2", and "3" in the figures). In addition, the well that did hit bedrock (marked "4" in the figures) is also in agreement with the model. The fifth water well (marked "5" in the figures), however, has a poor match. This shallow well (~50 m deep) did not encounter bedrock yet resides in an area where the depth-to-bedrock model predicts a near surface sediment thickness <10 m. As a result, a "divot" of sediments was artificially inserted into the geology model at the location of the 50 m deep water well.

In general, the geologically constrained density inversion model for cross-section D-D' shows a good match between the reference and inversion results (Figs. A1-3 and A1-4, middle and lower panels). The density inversion model results with both the high-and low-density colour schemes show relatively uniform density values in the Shonektaw and Snowcap rock units. For example, in section D-D' the model density of the Shonektaw unit varies from 2770–2860 kg/m^3 (compared to the reference value of 2840 kg/m^3). Similarly, the Snowcap rock unit shows model densities from 2550–2660 (compared to the reference value of 2640 kg/m^3). Therefore, the top-of-bedrock surface is well constrained provided the assumptions that went into the modelling are correct.

Depth-to-bedrock map

The 3D gravity inversion model results were used to construct a depth-to-bedrock map for the entire 3.1 km x 2.3 km area around the Village of Teslin (Fig. A1-5). This depth-to-bedrock map estimates the thickness of near surface sediments on top of the bedrock. The map is most accurate within the area covered by the tightly spaced gravity measurements. Outside of this area, the depth-to-bedrock map should only be used as a rough guide. In fact, on the west-central side of map (just north of the Alaska Highway), there appears to be a steep-sided pinnacle in the bedrock surface—this is likely an artifact of the modelling process because it occurs on the western edge of the tightly spaced gravity measurements (*i.e.* there is not data to the west of the pinnacle to constrain the actual shape of the top of the bedrock). The depth-to-bedrock map is unable to predict sediment thicknesses less than 10 m because that is the thickness of the smallest cell size used in the modelling. It should be noted that bedrock is exposed on the northwest side of the Village of Teslin. This outcrop is in a portion of the depth-to-bedrock map showing very thin sediment cover. Overall, the greatest thicknesses of sediment near the Village of Teslin is most likely to be found in the south as well as in the west (near the Alaska Highway). To the east of the village, the sediment layer is expected to be quite thin.

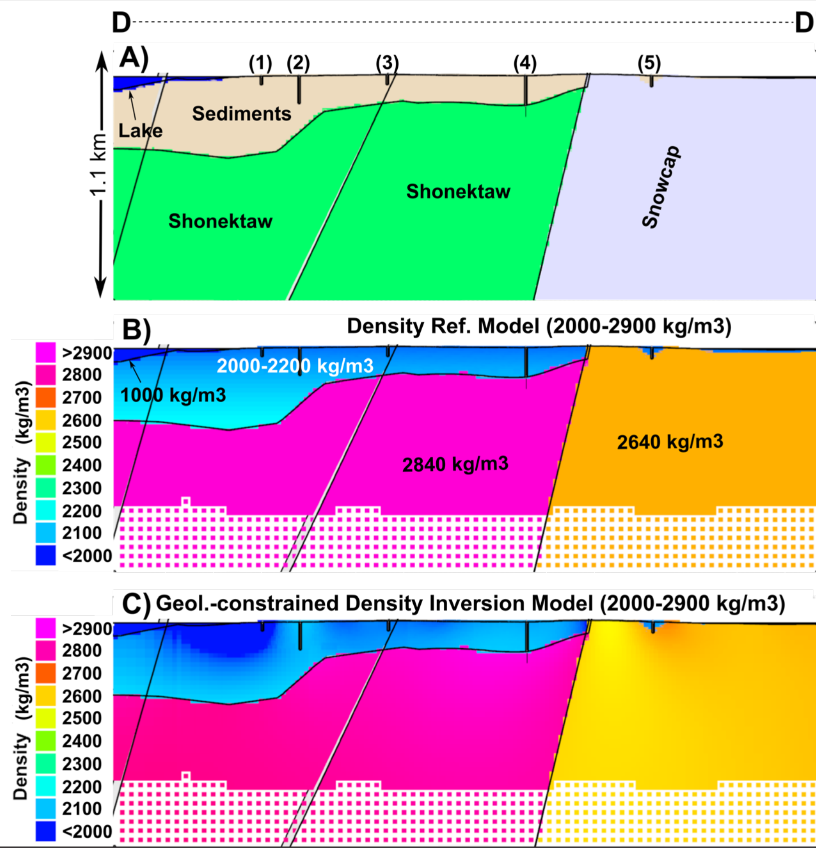

Figure A1-3. *Geology and density cross-sections along D-D' through five water wells using the lower density colour ramp (2000–2900 kg/m³).* ***A)*** *Reference geology model with rock units labeled and water wells numbered as follows: (1) Teslin Tlingit FN Well, Lot 154 (38 m deep); (2) Well WTH No. 1–87 (122 m deep); (3) TTFN Administration Building Well (45 m deep); (4) BOT TW10-01 well (182 m deep; hit bedrock at 130 m); (5) Mukluk Annie's Restaurant well (49 m deep). Teslin Lake Motors well also lies on this cross-section, about 165 m west of the Mukluk Annie's well; however, it is not shown here because there is no public information for the well.* ***B)*** *Reference rock density model used as constraints on the modelling.* ***C)*** *Rock density distribution returned by the 3D gravity inversion modelling that honours the gravity data. The colour scale for (B) and (C) is at the lower end of the density range (2000–2900 kg/m³) to visualize the lower density sedimentary rocks in the area. See text for further explanation.*

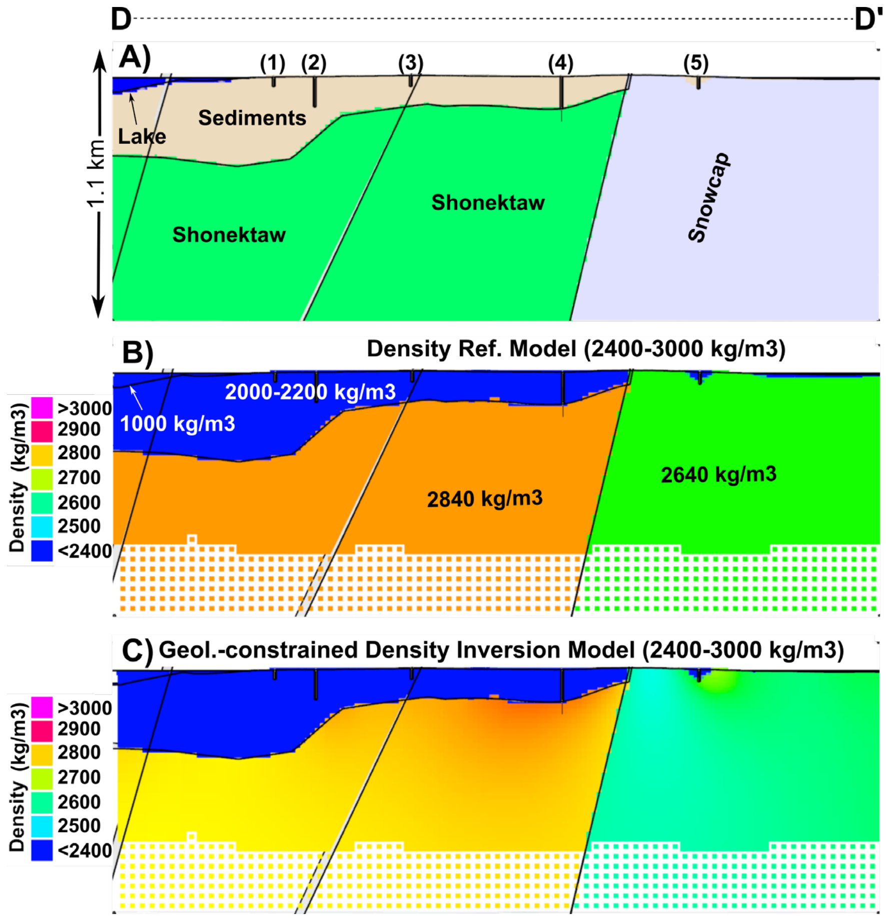

Figure A1-4. *Geology and density cross-sections along D-D' through five water wells using the higher density colour ramp (2400–3000 kg/m³).* ***A)*** *Reference geology model with rock units labeled and water wells numbered as in Figure A1-3.* ***B)*** *Reference rock density model used as constraints on the modelling.* ***C)*** *Rock density distribution returned by the 3D gravity inversion modelling that honours the gravity data. The colour scale for (B) and (C) is at the higher end of the density range (2400–3000 kg/m³) to visualize the higher density bedrock lithologies in the area. See text for further explanation.*

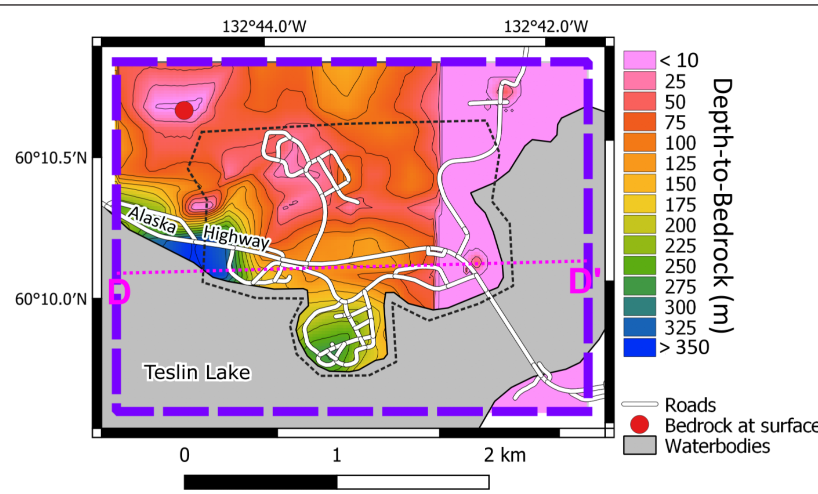

Figure A1-5. *Depth-to-bedrock map in the Village of Teslin area. Contour intervals are 25 m. Depth-to-bedrock is not shown under Teslin Lake (grey area). Black dotted line encloses the area with tightly spaced gravity measurements made 100 m apart. The area inside the black dotted line is a region of higher confidence in the depth-to-bedrock estimates because of the higher density gravity data.*

Appendix 2: Statement of qualifications

This report has been prepared by Jeffrey B. Witter, Principal Geoscientist at Innovate Geothermal Ltd. Dr. Witter holds an undergraduate degree in geophysics as well as Master's and Ph.D. degrees in geology. He has eighteen years of experience as an exploration geologist/geophysicist in the natural resource industry with more than half of that time committed specifically to geothermal exploration and resource evaluation. He is a registered professional geoscientist in the province of British Columbia (Canada) and is a member of Engineers and Geoscientists of British Columbia (EGBC). EGBC has a defined and enforceable Code of Ethics which Dr. Witter agrees to abide by. Dr. Witter has been engaged as a Consultant by the Yukon Geological Survey but holds no financial interest in any geothermal energy project in Yukon.

Dated in Vancouver, British Columbia, Canada this 1st day of June 2023

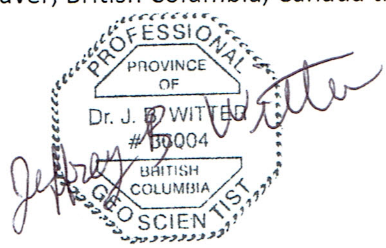

Jeffrey B. Witter Ph.D., PGeo (Province of British Columbia, No. 36004)

Appendix 3: Teslin gravity data and report; Aurora Geosciences

This appendix is only available digitally. The files are included in a .zip file that accompanies this document, and are available from https://data.geology.gov.yk.ca

Appendix 4: Additional geoscience data files

This appendix is only available digitally. The files are included in a .zip file that accompanies this document, and are available from https://data.geology.gov.yk.ca

All .shp, .dxf, and .tif files, as well as 3D block models in .txt file format are georeferenced to UTM NAD83 zone 8 (EPSG: 26908).

File name	File description
Teslin_gridded_CBA_gravity_data.tif	Complete Bouguer Anomaly gravity data with 2.67 g/cm^3 terrain correction density, gridded with 100 m cell size (units: mGal)
Teslin_gridded_CBA-THG_gravity_data.tif	Complete Bouguer Anomaly gravity data with 2.67 g/cm^3 terrain correction density, gridded with 100 m cell size, upward continued by 100 m, with Total Horizontal Gradient filter applied (units: mGal/m)
Teslin_gridded_TMI-RTP_magnetic_data.tif	Total Magnetic Intensity data with reduced-to-pole applied, gridded with 100 m cell size (units: nT)
Teslin_gridded_TMI-RTP-THG_magnetic_data.tif	Total Magnetic Intensity data with reduced-to-pole applied, gridded with 100 m cell size, and with Total Horizontal Gradient filter applied (units: nT/m)
Teslin_Structural_Interpretation_2023.shp	Geologic structures inferred from analysis of gravity and magnetic data
Teslin_Depth-to-Bedrock_map.tif	Map of the estimated depth below the ground surface to the top of bedrock (units: metres)
Teslin_LargeModelVolume_CornerPts.csv	Corner points of the 10.5 km x 10.5 km x 4.5 km model volume used in this study
Teslin_SmallModelVolume_CornerPts.csv	Corner points of the 3.2 km x 2.3 km x 1.1 km model volume for the depth-to-bedrock study
Teslin_3D_Structural_Framework.dxf	3D fault surfaces interpreted in this study
Teslin_Large_Density_Inversion_Model.txt	Geologically constrained density inversion 3D model output for the large model volume
Teslin_Large_Density_Reference_Model.txt	Density reference model used as geological constraints in the large model volume
Teslin_Large_MagSusc_Inversion_Model.txt	Geologically constrained magnetic susceptibility inversion 3D model output for the large model volume
Teslin_Large_MagSusc_Reference_Model.txt	Magnetic susceptibility reference model used as geological constraints in the large model volume
Teslin_Small_Density_Inversion_Model.txt	Geologically constrained density inversion 3D model output for the small model volume
Teslin_Small_Density_Reference_Model.txt	Density reference model used as geological constraints in the small model volume

Yukon Geological Survey
Energy, Mines and Resources
Government of Yukon